UNIVERSIDADE DO VALE DO RIO DOS SINOS - UNISINOS
UNIDADE ACADÊMICA DE PESQUISA E PÓS-GRADUAÇÃO
PROGRAMA DE PÓS-GRADUAÇÃO EM GEOLOGIA
NÍVEL MESTRADO

DISSERTAÇÃO DE MESTRADO

The shelf edge: characterization and significance of the shelf-slope break threshold for the infilling of the mid-Jurassic Neuquén Basin, Argentina

NÌVEL MESTRADO

The shelf edge: characterization and significance of the shelf-slope break threshold for the infilling of the mid-Jurassic Neuquén Basin, Argentina

Flávio Norberto de Almeida Júnior

São Leopoldo
2020

UNIVERSIDADE DO VALE DO RIO DOS SINOS - UNISINOS
UNIDADE ACADÊMICA DE PESQUISA E PÓS-GRADUAÇÃO

PROGRAMA DE PÓS-GRADUAÇÃO EM GEOLOGIA

Nome do Autor: Flávio Norberto de Almeida Júnior

Título: "The shelf edge: characterization and significance of the shelf-slope break threshold for the infilling of the Mid-Jurassic Neuquén Basin, Argentina"

Nível: Mestrado

Data de Defesa: 13/04/2020

E-mail de Contato do Autor: flavionorbertoajr@gmail.com

Este documento aborda a caracterização sedimentológica e estratigráfica de depósitos sedimentares de borda de plataforma, Jurássico da Bacia de Neuquén, Argentina, em um contexto mais amplo de evolução das margens de plataformas desenvolvidas em bacias sedimentares de ambiente marinho profundo.

Orientador: Prof. Dr. Paulo Sérgio Gomes Paim

Coorientador: Prof. Dr. Ronald Steel (University of Texas at Austin)

A447s Almeida Júnior, Flávio Norberto de.
The shelf edge : characterization and significance of the shelf-slope break threshold for the infilling of the mid-Jurassic Neuquén Basin, Argentina / Flávio Norberto de Almeida Júnior. – 2020.
[58] f. : il. ; 30 cm.

Dissertação (mestrado) – Universidade do Vale do Rio dos Sinos, Programa de Pós-Graduação em Geologia, 2020.
"Orientador: Prof. Dr. Paulo Sérgio Gomes Paim ; coorientador: Prof. Dr. Ronald Steel".

1. Geologia. 2. Clinoformas. 3. Borda da plataforma. 4. Quebra talude-plataforma 5. Bacia de Neuquén. I. Título.
CDU 55

Dados Internacionais de Catalogação na Publicação (CIP)
(Bibliotecário: Flávio Nunes – CRB 10/1298)

ACKNOWLEDGEMENTS

I would like to express my sincere gratitude to my research supervisor, Professor Paulo Sérgio Gomes Paim, for giving me the opportunity to do research and providing invaluable guidance throughout this research. Unisinos University represented a turning point in my career, where for the first time in my own country, I was treated as a professional and my research work was technically valued. My heartfelt thanks is extended to professors, employees and research colleagues.

Professor Ronald Steel and Dr. Cornel Olariu, my co-supervisors, are particularly thanked here. Prof. Steel's invitation to join his research group, even barely knowing me from pointed academic references, represented my first research opportunity in the field of sedimentary geology. Over the last few years, his Dynamic Stratigraphy Workgroup covered all the financial costs of my research work, provided me with state-of-the-art training and guidance in several topics of sedimentary geology, but most importantly, the whole group trusted and supported my research work. These words are not enough to express my lifetime gratitude. The kind words are extended to my fieldwork comrades and research collaborators MSc. Yuqian (Philomena) Gan and MSc. Gabriel Giacommone.

The present thesis is dedicated to my parents and brothers, my grandparents, girlfriend, the good and (mainly) crazy old friends and, most importantly, to Brazilian citizens who are the ultimate responsible for keeping science alive in the darkness.

What's next…?

"Compañeros, el viaje continúa con la misma brújula, con el mismo destino, pero con una nave más grande"

Luis Carlos Galán

INDEX

ABSTRACT

Sedimentary wedges that build out from the margin of deep-water basins often exhibit large-scale (hundreds of meters), topset-foreset clinoform geometries. Deepwater basins therefore have a shelf-margin morphology of flat to gently sloping shelf, together with a steeper deepwater slope (1-4 degrees) and a gently sloping to flat basin floor. The two inflection points along the margin morphology are the shelf-slope break (or shelf edge), and the toe of slope break. The significance of such clinoformal patterns in stratigraphy is that they demonstrate the time equivalence of the sandy shallow-water shelf deposits with the respective muddy deepwater slope deposits, and allow the position of the shelf edge or the shelf-slope break and the toe of slope break to be pinpointed in the stratigraphy. This typical shelf-slope-basin floor clinoform geometry is easily recognizable in seismic data sets, but difficult to determine (when not supported by seismic) in outcrops because shelf-margin clinothems in exhumed basin are generally destroyed due to erosion and deformation. Only few places clinoforms can be recognized in outcrops, such as, for example, the Eocene Central Basin of Spitsbergen (Norway), where the exposures are large and continuous with sandstones punctuating the hundreds of meters muddy slope clinoforms. Although seismic data allow shelf-slope-basin floor deposits to be constrained within chronostratigraphic intervals, they do not provide the bed-scale resolution inherent in the refinement of geological models. Outcrop analogue studies provide the finer-scale resolution needed, but these are not without problems too because co-genetic shelf-slope-basin floor deposits cannot often be time-correlated in outcrops. It implies that little is known about the character of the linkage between the shallow-water shelf and the associated deep-water depositional systems, since this transition has rarely been seen in outcrop where the downslope facies changes can be described and quantified. The mid-Jurassic deposits of Challaco-Las Lajas-Los Molles formations of southern Neuquén Basin, in La Jardinera area, fill the basin by means of building shelf-slope-basin floor clinoforms. Exceptional outcrops expose the hundreds of meters thick clinoforms, and thus, enabled a time- correlation between the shallow-water shelf and the deepwater depositional systems, and the character of this transition to be described and quantified. This study provided a three-dimensional, bed-scale and architectural model for the shelf edge rollover deposits that can be used as an analogue for subsurface predictability of deepwater reservoir presence and de-risking of prospects in similar settings. This conceptual paleographic model bring important contributions to improve our understanding of how sediment moves from shelf to deepwater areas of shelf margins.

Key words: Clinoforms, shelf edge, shelf-slope break, Neuquén Basin

1. INTRODUCTION

The present master's research component was designed to investigate in detail some key sedimentological and stratigraphic aspects of the Lower-Middle Jurassic shelf edge (or shelf-slope break) deposits cropping out in the southernmost Neuquén Basin, Argentina, aiming at enhancing the assessment of sub-seismic reservoir presence and de-risking of prospects in deep-water basins. This field-based study used the principles of lithostratigrahic logging and facies analysis as an essential tool for better understanding the nature of shelf edge depositional environments and its processes. The fundamental aspects tackled within this master's research framework include:

(i) Reconstruction of clinoform stratigraphy in outcrops – with detailed depositional strike and dip architecture of the Lower-Middle Jurassic Margin clinoforms;

(ii) The three-dimensional (i.e. depositional strike and dip sections), bed-scale facies and architecture model for shelf edge depositional paleoenvironments – reconstruction of coeval facies belts, their depositional processes and their relative shifts or lateral migration with time;

(iii) Process regime at the shelf edge (tidal, wave and river currents interaction) and its implication for sediment transfer (i.e. sand and pebbles) onto deep-water areas of shelf margins;

(iv) The stratigraphic relation between outermost shallow-water shelf and uppermost deepwater slope depositional systems;

Three fieldwork campaigns have been conducted in Argentina, from 2017 to 2019, in cooperation with the Dynamic Stratigraphy Workgroup, University of Texas at Austin, who generously covered the total financial costs inherent to the completion of this field-based research work. The research project was financially supported by Shell Houston, YPF and PlusPetrol. Unisinos University has provided with essential academic support through its Postgraduate Program in Geology, where data analysis and scientific writing have been performed under the supervision of Professor Paulo Sérgio Gomes Paim. This research builds further on previous work developed by Paim and others (2008; 2011).

1.1. Why is studying the shelf edge important?

The shelf-slope break is located where the shelf rolls over into the slope, along the line where the rate of increase in shelf gradient reaches a maximum (Southard and

Stanley, 1976; Olariu and Steel, 2009; Helland-Hansen et al., 2012). This shelf-slope break (or shelf edge) is analogous to the transition from the continental shelf to the continental slope, and is the 'staging area' for the delivery of sand that becomes the deepwater reservoirs of the basin (Johannessen and Steel, 2005). A thorough characterization of the shelf edge is of great interest because of the following reasons:

(i) It marks a threshold between the dominantly wave, tidal, shelf currents or delta (fluvial derived) deposits of shelf and the sediment-gravity driven deposits (e.g., turbidites) of the deepwater slope.

(ii) It also records a change from fairly sand-rich shelf deposits to mud-prone deepwater slope deposits.

(iii) The sedimentological characterization of the shelf edge elucidates the mechanisms and processes driving shelf-edge sand into deepwater basins, thus providing analogue examples that allow a better prediction of subsurface deepwater reservoir presence and de-risking of prospects.

(iv) Through time, with successive cycles of sedimentation, the shelf edge of the basin migrates basinwards and the shelf widens, but the locus of the shelf edge migration in space is sensitive to sea-level change and to tectonic movements, and so a study of this stratigraphic level will, in fact, provide critical insights to these controls.

Although the shelf-slope break has been frequently identified on seismic data, it has only rarely been seen in outcrops where the downslope facies changes can be described and quantified (e.g., Laugier and Plink-Björklund, 2016). Therefore, the exact bed-scale character of this transition has rarely been documented. Consequently, there is currently a dearth of information on the detail of what happens within the broad shelf-slope rollover zone. Unless we understand the options for how sandy sediment enters this eventual shelf-slope transition, it is not easily predictable how grain size, facies and sediment volumes are partitioned during this last phase of the source-to-sink journey. The prediction as to whether significant sand volumes are likely to have by-passed the shelf is therefore important.

1.2. Objectives

The aim of this study is to develop a three-dimensional, bed-scale facies and architectural model for shelf edge deposits that can be used as:

(i) A *norm* with which local cases can be compared;

(ii) A *conceptual framework* and *guide* for future observations and for the analysis of the pattern of depositional processes characteristic of shelf-edge rollover sites and the corresponding deepwater slope depositional paleoenvironments;

(iii) An *analogue* for subsurface predictability of deepwater reservoir presence and de-risking of prospects.

This conceptual paleographic model should (at last) bring important contributions to improve our understanding of how sediment moves from shallow-water shelf onto deepwater areas of shelf margins.

2. DATA SET AND METHODOLOGY

2.1. Literature review

This first phase consisted on systematic literature review throughout the development of the master's thesis. The latter review included scientific articles published in peer-reviewed journals, both Doctoral and Master's theses, and also academic and industry reports from mostly Argentinian companies and research institutions.

2.2. Fieldwork – data acquisition

(i) Detailed centimeter- to decimeter-scale logging of vertical sedimentary successions (the study vertical interval is about 70 m), 100 m apart along the 10x20 km area, with a systematic recording of lithology, grain-size, primary and secondary sedimentary structures, the nature of bed boundaries, bed thicknesses, sand/mud ratio changes and bedforms architecture across the shelf edge boundary to produce lithostratigraphic logs.

(ii) Mapping of the shelf edge and the associated large-scale clinoform geometries. For defining individual clinothems, we began defining them on the topset area

(see Steel et al., 2019) where the shoreline sandstone units are upward-coarsening, laterally continuous and bounded by thick shales. The latter shales can be considered flat-lying surfaces, so they can be used as a datum to define gradient changes along the shelf-slope profile. The continued mapping of the slope reaches of the clinothems were done by (1) using top (muddy intervals) of some coarse-grained channelized deposits at the shelf edge that also persists as tongues and channels fills down throughout the muddy slope, (2) identifying the maximum flooding surfaces both below and above these sandstone tongues, and (3) further mapping (on satellite photos) and by walking out the downslope reaches of the clinothems. It allowed correlation between coeval depositional systems (see Olariu et al., 2019).

(iii) Paleocurrent readings have been measured from cross-beds, current ripple lamination, channel axes, sole marks and clast imbrication. Bedding plane attitudes (strike and dip) were also measured to restore tilted bedding planes to their original position.

(iv) Drone photography were taken and merged into high resolution photopanels (Agisoft PhotoScan), which were used to construct bedding diagrams (bedding architecture) and correlate between lithostratigraphic logs.

(v) Hundreds of georeferenced points of control were acquired walking along the main stratigraphic boundaries. It was prove to be essential for an accurate correlation of the major stratigraphic boundaries and also for the multi-scale architectural reconstruction of the shelf-edge deposits.

2.2.1. Data acquired

A total of *ca.* 2100 m of sedimentary sections were logged, coupled with 258 paleocurrent readings and "photopannel" bedding diagrams covering km-long outcrop belts oriented both along depositional strike and near-depositional dip, together with hundreds of georeferenced points of control acquired walking along the main stratigraphic boundaries.

2.3. Data analysis

(i) Development of detailed facies analysis and stratigraphic log correlation supported by a high-resolution DEM (*ca.* 0.5 m) and "photopannels".

Sedimentary facies were divided based on the distinctive aspects of rock units that form under a spectrum of physical conditions and reflect particular process or environment. Facies associations were further defined according to a grouping of spatially related and genetically coherent facies, both horizontally and vertically, and their position along the shelf-margin profile (i.e. shelf, slope and basin floor).

(ii) Paleocurrents directions were obtained after correcting the original readings by restoring the tilted bedding planes to their original position. An academic version of Stereonet 10 has been used for restoration, as the software provides a free-access tool for it.

(iii) Facies quantification and inferred process regime changes (tidal-, wave- and fluvial derived processes) at the shelf edge.

(iv) Quantification of grain size changes and general sand-mud partitioning from shallow to deepwater reaches across the shelf and uppermost slope segments of the clinothems.

(v) Scientific writing for peer reviewed journals

3. RESULTS

First-authored article (presented here as the main core of the Master's Thesis):

De Almeida Junior, FN, Steel, RJ, Olariu, C, Gan, Y, Paim, PSG. (2020) River-dominated and tide-influenced shelf-edge delta systems: coarse-grained deltas straddling the Early-Middle shelf-slope break and transforming downslope, Lajas-Los Molles formations, Neuquén Basin, Argentina. https://doi.org/10.1111/sed.12721

Journal: *Sedimentology* (Qualis CAPES: A1) – Published online

The paper is attached as appendix and comprises the main product of this master's thesis.

Reviewers:

Prof. Peter Burgess, University of Liverpool

Prof. Stephen Hubbard, University of Calgary

Prof. Massimiliano Guinassi

Co-authored articles (not included in this document, but developed concomitantly with the thesis):

Gan, Y, Steel, RJ, Olariu, C, **De Almeida, F**. Facies and architectural variability of sub-seismic slope-channel fills in prograding clinoforms, Mid-Jurassic Neuquén Basin, Argentina. *Basin Res*. 2019; 00: 1– 15. https://doi.org/10.1111/bre.12409

Olariu, C, Steel, RJ, Vann, NK,Tudor, EP, Shin, M, Winter, RR, Gan, Y, Jung, E, **Almeida Jr F**, Giacomone, G, Minisini, D, Brinkworth, W, Loss, ML, Inigo, J, Gutierrez, R.. Criteria for recognizing shelf-slope clinoforms in outcrop; Jurassic Lajas and Los Molles formations, S. Neuquén Basin, Argentina. *Basin Res*. 2019; 00: 1– 14. https://doi.org/10.1111/bre.12395

4. SOME KEY MISSING POINTS THAT WERE NOT INCLUDED IN THE PUBLISHED ARTICLE

Paim & others, (2008, 2011) and Olariu & others (2019) have recognized the co-genetic nature of Cuyo Group, which Challacó-Lajas-Los Molles are diachronous lithostratigraphic formations and partly proximal-distal equivalents with one another respectively as alluvial-to-shelf, slope and basin floor deposits. However, both facies models present substantial differences. The work presented here, i.e. Almeida Júnior & others (2020), converges with the clinoform stratigraphy model proposed by Olariu & others (2019). Almeida Júnior & others (2020) provided a more detailed stratigraphic characterization of clinoform sets and clinothems, but lacked on providing detailed comparison with the previous facies model proposed by Paim & others (2008). The following two key contrasting points of view characteristic of each model (Almeida Júnior & others, 2020; and Paim & others, 2008) are here summarized for further discussion during the thesis' formal presentation:

i) Paim & others, (2008) have interpreted a 3rd order sequence boundary between Lajas and Los Molles formations. By including a sequence boundary of proximal-distal continuity, the authors interpreted that Lajas (topset/shelf) and Los Molles (foreset/slope) deposits are not coeval in La Jardinera section.

Olariu & others, (2019) and Almeida Júnior & others (2020), contrastingly, have mapped and reconstructed clinoform stratigraphy, thus interpreting that Lajas topset/shelf and Los Molles foreset/slope deposits are coeval and can be time-torrelated in La Jardinera study area.

ii) Paim & others (2008) have placed at the base of the coarse-grained, river channel-fill deposits, which can be seen to downcut the underlying lower delta front sandstones within individual shallowing and coarsening upwards units or "parasequences", as a lower-order sequence boundary representing high-frequency base level changes resulting from falling in relative sea level. The interpretation implies incision and extension of river mouths across shelves, which would then result in subaerial shelf exposure and complete sediment bypass. Channels are then considered to have been filled during subsequent transgression.

Almeida Júnior & others (2020), on the other hand, interpreted the same aforementioned channelized, coarse-grained units as being representative of delta distributary-channel fill deposits, primarily not isolated from the deltas. The authors interpreted these distributary channels as being also depositional during regression, but not being exclusively bypassing systems. The lack of evidence for subaerial exposure in these deposits, which has been not demonstrated by Paim & others (2008), together with the overall evidence of tidal reworking and the marine trace fossils presence (e.g. *Siphonicnus*), do not suggest prolonged periods of subaerial shelf exposure. Although base level changes (eustatic and tectonic) are considered, authors have also argued that regressions can been also driven mainly by climate and severe river flooding operating on a faster time-scale than base-level changes.

5. CONCLUSION REMARKS

The Lower-Middle Jurassic Lajas and Los Molles formations in the Arroyo La Jardinera area, southern Neuquén Basin, Argentina, represent an unusual and well-exposed example of shelf-edge deltaic deposits. The results obtained through the development of this master's research represent an important contribution to the understanding of the role of shelf-edge rollover zone depositional systems for the

evolution of shelf margins in deep-water basins. This contribution documents one-of-kind example of coarse-grained (mostly conglomeratic) shelf-edge delta systems, tying bed-scale facies and architecture data to a mapped seismic-scale shelf-margin morphology, thus providing outcrop analogue data for the characterization of shelf-edge delta systems in the subsurface.

The main findings of this master's research include:

- The unusual coarseness of shelf-edge deltaic deposits, as well as the strong tidal influence in the inter-distributary or distributary-abandoned areas.
- The interplay between flood tides and river currents, an autogenic process within shoreline depositional systems, was not only efficient transporting coarse-grained sediment onto the deep-water areas, but seems to have also modulated such transport through preferential routes (i.e. main distributary channel fairways) on the outer-shelf to shelf edge and down onto the slope systems.
- Lack of slumped and collapsed strata at the shelf edge, which suggests continuity between subaqueous river channels and deepwater slope channels. The latter is supported by a downslope flow transformation seen in individual clinothems – i.e. shelf-edge distributary channel-fills show a downslope change from stratified conglomerates with relatively well-sorted, clast-supported gravel with minimal sand matrix (as common in river channels) to poorly sorted, mainly sand matrix-supported, unstratified debrites and high-density turbidites of slope settings.
- Shelf to slope sediment transport in shelf-edge deltas can be seen to be primarily driven by the interplay between: (i) base-level changes (eustatic or tectonic) and (ii) regressions driven mainly by climatic and severe river flooding, operating on a faster time-scale than base-level changes.

This research has been published in the *Sedimentology Journal* (International Association of Sedimentologists), the international leader in its field, thus fulfilling all the requirements for the completion of a Master's Degree in Geology at Unisinos University.

REFERENCE

Ainsworth, R. B., Vakarelov, B. K., Lee, C., MacEachern, J. A., Montgomery, A. E., Ricci, L. P., and **Dashtgard, S. E.** (2015) Architecture and evolution of a regressive, tide-influenced marginal marine succession, Drumheller, Alberta, Canada. *Journal of Sedimentary Research*, **85(6)**, 596-625.

Archer, A. W., and **Hubbard, M. S**. (2003) Highest tides of the world. *Special Papers-Geological Society of Ameica*, 151-174.

Brinkworth, W., Vocaturo, G., Loss, M. L., Giunta, D., Mortaloni, E., & **Massaferro, J.** (2017). Integración regional de subsuelo orientado a la exploración y desarrollo de Grupo Cuyo, Cuenca Neuquina. *Tucumán: Congreso Geológico Argentino.*

Burgess, P. M., & **Hovius, N**. (1998). Rates of delta progradation during highstands: consequences for timing of deposition in deep-marine systems. *Journal of the Geological Society*, **155(2)**, 217-222.

Burgess, P. M., Flint, S., and **Johnson, S.** (2000) Sequence stratigraphic interpretation of turbiditic strata: an example from Jurassic strata of the Neuquén basin, Argentina. *Geological Society of America Bulletin*, **112(11)**, 1650-1666.

Carter, R. M. (1975). A discussion and classification of subaqueous mass-transport with particular application to grain-flow, slurry-flow, and fluxoturbidites. *Earth-Science Reviews*, **11(2)**, 145-177.

Carvajal, C.R. and **Steel, R.J.** (2006) Thick turbidite successions from supply-dominated shelves during sea-level highstand. *Geology*, **34**, 665-668.

Covault, J.A., Normark, W.R., Romans, B.W. and **Graham, S. A.** (2007) Highstand fans in the California borderland: The overlooked deep-water depositional systems. *Geology,* **35**, 783-786.

Covault, J. A., Romans, B. W., and **Graham, S. A.** (2009) Outcrop expression of a continental-margin-scale shelf-edge delta from the Cretaceous Magallanes Basin, Chile. *Journal of Sedimentary Research*, **79(7)**, 523-539.

Cummings, D. I., Arnott, R. W. C., and **Hart, B. S.** (2006) Tidal signatures in a shelf-margin delta. *Geology*, **34(4)**, 249-252.

Dakin, N., Pickering, K. T., Mohrig, D., and **Bayliss, N. J.** (2013) Channel-like features created by erosive submarine debris flows: field evidence from the Middle Eocene Ainsa Basin, Spanish Pyrenees. *Marine and Petroleum Geology*, **41**, 62-71.

Dalrymple, R. W., and **Rhodes, R. N.** (1995) Estuarine dunes and bars. In *Developments in sedimentology*, **53**, 359-422. Elsevier.

Dalrymple, R. W., & **Choi, K.** (2007). Morphologic and facies trends through the fluvial–marine transition in tide-dominated depositional systems: a schematic framework for environmental and sequence-stratigraphic interpretation. *Earth-Science Reviews*, **81(3-4)**, 135-174.

Dixon, J. F., Steel, R. J., and **Olariu, C.** (2012) River-dominated, shelf-edge deltas: delivery of sand across the shelf break in the absence of slope incision. *Sedimentology*, **59(4)**, 1133-1157.

Dixon, J. F., Steel, R. J., and **Olariu, C.** (2012) Shelf-edge delta regime as a predictor of deep-water deposition. *Journal of Sedimentary Research*, **82(9)**, 681-687.

Dzulynski, S., Ksiazkiewicz, M., & **Kuenen, P. H.** (1959). Turbidites in flysch of the Polish Carpathian Mountains. *Geological Society of America Bulletin*, **70(8)**, 1089-1118.

Dzulynski, S. (1965). New data on experimental production of sedimentary structures. *Journal of Sedimentary Research*, **35(1)**, 196-212.

Fleming, R. H., & **Revelle, R.** (1939). Recent Marine Sediments. *Amer. Soc. Petrol. Geol., Tulsa, Oklahoma*.

Franzese, J. R., and **Spalletti, L. A.** (2001) Late Triassic–early Jurassic continental extension in southwestern Gondwana: tectonic segmentation and pre-break-up rifting. *Journal of South American Earth Sciences*, **14(3)**, 257-270.

Franzese, J., Spalletti, L., Pérez, I. G., and **Macdonald, D**. (2003) Tectonic and paleoenvironmental evolution of Mesozoic sedimentary basins along the Andean foothills of Argentina (32–54 S). *Journal of South American Earth Sciences*, **16(1)**, 81-90.

Galloway, W. E. (1998). Siliciclastic slope and base-of-slope depositional systems: component facies, stratigraphic architecture, and classification. *AAPG bulletin*, **82(4)**, 569-595.

Gan, Y. P., Steel, R. J., Olariu, C., & **De Almeida, F.** (2019). Facies and architectural variability of sub-seismic slope-channel fills in prograding clinoforms, Mid-Jurassic Neuquén Basin, Argentina. *Basin Research*. Online.

Gobo, K., Ghinassi, M., & **Nemec, W.** (2015). Gilbert-type deltas recording short-term base-level changes: Delta-brink morphodynamics and related foreset facies. *Sedimentology*, **62(7)**, 1923-1949.

Gomis-Cartesio, L.E, Poyatos-More, M., Flint, S.S., Hodgson, D.M., Brunt, R.L. and **Wickens, H.V.** (2016) Anatomy of a mixed-influence shelf-edge delta, Karoo Basin, South Africa. *Geological Soviety Special Publications,* **444 (1),** 393-418.

Gugliotta, M., Flint, S. S., Hodgson, D. M., and **Veiga, G. D.** (2015) Stratigraphic record of river-dominated crevasse subdeltas with tidal influence (Lajas Formation, Argentina). *Journal of Sedimentary Research*, **85(3)**, 265-284.

Gulisano, C. A., and **Pando, G. A.** (1981) Estratigrafía y facies de los depósitos jurásicos entre Piedra del Águila y Sañicó, Departamento Collón Curá, Provincia del Neuquén. In *Congreso Geológico Argentino*, **8**, 553-577.

Gulisano, C. A., Gutiérrez Pleimling, A. R., and **Digregorio, R. E.** (1984) Esquema estratigráfico de la secuencia jurásica del oeste de la provincia del Neuquén. In *Congreso Geológico Argentino* **(9)**, 236-259.

Hernández-Molina, F. J., Fernández-Salas, L. M., Lobo, F., Somoza, L., Díaz-del-Río, V., and **Dias, J. A**. (2000) The infralittoral prograding wedge: a new large-scale progradational sedimentary body in shallow marine environments. *Geo-Marine Letters*, **20(2)**, 109-117.

Hoitink, A. J. F., Wang, Z. B., Vermeulen, B., Huismans, Y., & **Kästner, K.** (2017). Tidal controls on river delta morphology. *Nature geoscience*, **10(9)**, 637-645.

Houseknecht, D. W., **Bird, K. J**., and **Schenk, C. J.** (2009) Seismic analysis of clinoform depositional sequences and shelf-margin trajectories in Lower Cretaceous (Albian) strata, Alaska North Slope. *Basin Research*, **21(5)**, 644-654.

Howell, J. A., Schwarz, E., Spalletti, L. A., & **Veiga, G. D.** (2005). The Neuquén basin: an overview. *Geological Society, London, Special Publications*, **252(1)**, 1-14.

Hubbard, S. M., **Fildani, A.**, **Romans, B. W**., **Covault, J. A**., and **McHargue, T. R.** (2010) High-relief slope clinoform development: insights from outcrop, Magallanes Basin, Chile. *Journal of Sedimentary Research*, **80(5)**, 357-375.

Hubbard, S. M., Covault, J. A., Fildani, A., & **Romans, B. W.** (2014). Sediment transfer and deposition in slope channels: deciphering the record of enigmatic deep-sea processes from outcrop. *Bulletin*, *126*(5-6), 857-871.

Introcaso, A., Pacino, M. C., and **Fraga, H.** (1992) Gravity, isostasy and Andean crustal shortening between latitudes 30 and 35 S. *Tectonophysics*, **205(1-3)**, 31-48.

Johannessen, E.P. and **Steel, R.J.** (2005) Shelf-margin clinoforms and prediction of deepwater sands. *Basin Res.,* **17**, 521-550.

Jones, G. E., Hodgson, D. M., and **Flint, S. S**. (2015) Lateral variability in clinoform trajectory, process regime, and sediment dispersal patterns beyond the shelf-edge rollover in exhumed basin margin-scale clinothems. *Basin Research*, **27(6)**, 657-680.

Kenyon, N. H., Belderson, R. H., Stride, A. H., & **Johnson, M. A.** (1981). Offshore tidal sand banks as indicators of net sand transport and as potential deposits. *Holocene Marine Sedimentation in the North Sea Basin*, **5,** 257-268.

Kim, Y., Kim, W., Cheong, D., Muto, T., and **Pyles, D. R.** (2013) Piping coarse-grained sediment to a deep water fan through a shelf-edge delta bypass channel: Tank experiments. *Journal of Geophysical Research: Earth Surface*, **118(4)**, 2279-2291.

Kim,H.J., Mallea, M., Gutiérrez, R. and **Malone, P.,** (2014) Exploracion del Gr. Cuyo Jurasico en Bloques Maduros de la Dorsal Huincul – puesto touquet y el Porvenir, Quenca Neuquena. . IX Congreso de Exploración y Desarrollo de Hidrocarburos, Mendoza-Argentina, **2**, pag. 71-93.

Kochhann, K. G. D., Baecker-Fauth, S., Pujana, I., da Silveira, A. S., and **Fauth, G.** (2011) Toarcian–Aalenian (Early–Middle Jurassic) radiolarian fauna from the Los Molles Formation, Neuquén Basin, Argentina: Taxonomy and paleobiogeographic affinities. *Journal of South American Earth Sciences*, **31(2-3)**, 253-261.

Kurcinka, C., Dalrymple, R. W., & **Gugliotta, M.** (2018). Facies and architecture of river-dominated to tide-influenced mouth bars in the lower Lajas Formation (Jurassic), Argentina. *AAPG Bulletin*, *102*(5), 885-912.

Laugier, F. J., and **Plink-Björklund, P**. (2016) Defining the shelf edge and the three-dimensional shelf edge to slope facies variability in shelf-edge deltas. *Sedimentology*, **63(5)**, 1280-1320.

Legarreta, L. and **Gulisano, C.A.** (1989) Análisis estratigráfico secuencial de la Cuenca Neuquina (Triásico superior-Terciario inferior, Argentina). *In*: Chebli, G and Spalletti, L. (eds) Cuencas Sedimentarias Argentinas. *Serie Correlación Geológica, Universidad Nacional de Tucumán,* **6,** 221-243.

Legarreta, L. and **Uliana, M.A.** (1991) Jurassic-Cretaceous marine oscillations and geometry of back arc basin fill, Central Argentine Andes. *In*: Macdonald, D.I.M. (ed.) Sedimentation, Tectonics and Eustasy- Sea-level Changes at Active Margins. *International Association of Sedimentologists, Special Publications,* **12,** 429-450.

Legarreta, L., and **Uliana, M. A**. (1996) The Jurassic succession in west-central Argentina: stratal patterns, sequences and paleogeographic evolution. *Palaeogeography, Palaeoclimatology, Palaeoecology*, **120(3-4)**, 303-330.

Leuven, J. R., van Maanen, B., Lexmond, B. R., van der Hoek, B. V., Spruijt, M. J., & **Kleinhans, M. G.** (2018). Dimensions of fluvial-tidal meanders: Are they disproportionally large?. *Geology*, **46(10)**, 923-926.

Liu, Z. X. (1997). Yangtze Shoal—a modern tidal sand sheet in the northwestern part of the East China Sea. *Marine Geology*, **137(3-4)**, 321-330.

Longhitano, S. G., **Mellere, D., Steel, R. J.,** & **Ainsworth, R. B.** (2012). Tidal depositional systems in the rock record: a review and new insights. *Sedimentary Geology*, **279**, 2-22.

Lowe, D. R. (1982) Sediment gravity flows: II Depositional models with special reference to the deposits of high-density turbidity currents. *Journal of Sedimentary Research*, **52(1)**, 279-297.

Manceda, R. and **Figueroa, D.** (1995) Inversion of the Mesozoic Neuquén rift in the Malargüe fold and thrust belt, Mendoza, Argentina. *In:* Tankard, A.J., Suaréz Soruco, R.

and Welsink, H.J. (eds) *Petroleum Basins of South America. AAPG Memoirs,* **62,** 369-382.

McIlroy, D., Flint, S., Howell, J. A., and **Timms, N**. (2005) Sedimentology of the tide-dominated Jurassic Lajas Formation, Neuquén Basin, Argentina. *Geological Society, London, Special Publications*, **252(1)**, 83-107.

Mellere, D., Plink-Björklund, P. and **Steel, R.** (2002) Anatomy of shelf deltas at the edge of a prograding Eocene shelf margin, Spitsbergen. *Sedimentology,* **49**, 1181-1206.

Mellere, D., Breda, A., Steel, R. J., Roberts, H. H., Rosen, N. C., Fillon, R. H., and **Anderson, J. B.** (2003) Fluvially-incised shelf-edge deltas and linkage to upper-slope channels (Central Tertiary Basin, Spitsbergen). *Global significance and future exploration potential: Gulf Coast Section-SEPM Special Publication*, **23**, 231-266.

Mitchum Jr, R. M., Vail, P. R., and **Thompson III, S**. (1977) Seismic stratigraphy and global changes of sea level, Part 2. The depositional sequence as a basic unit for stratigraphic analysis; Am. A, **26**, 53-62.

Moscardelli, L., Wood, L., and **Mann, P.** (2006) Mass-transport complexes and associated processes in the offshore area of Trinidad and Venezuela. *AAPG bulletin*, **90(7)**, 1059-1088.

Moss-Russell, A.C. (2009) The stratigraphic architecture of a prograding shelf-margin delta in outcrop, the Sobrarbe Formation, Ainsa Basin, Spain. Master's Thesis. Colorado School of Mines, 192 pp.

Nemec W. and **Steel**, **R. J.** (1984) "Alluvial and Coastal Conglomerates: Their Significant Features and Some Comments on Gravelly Mass-Flow Deposits," In: E. H. Koster and R. J. Steel, Eds. Sedimentology of Gravels and Conglomerates, *Canadian Society of Petroleum Geologists Memoir* **10**, 1984, pp. 1-31.

Olariu, C., Steel, R.J., Dalrymple, R.W. and **Gingras, M.K.** (2012) Tidal dunes versus tidal bars: The sedimentological and architectural characteristics of compound dunes in a tidal seaway, the lower Baronia Sandstone (Lower Eocene), Ager Basin, Spain. *Sed. Geol.,* **279,** 134-155.

Olariu, M. I., Olariu, C., Steel, R. J., Dalrymple, R. W., and **Martinius, A. W.** (2012) Anatomy of a laterally migrating tidal bar in front of a delta system: Esdolomada Member, Roda Formation, Tremp-Graus Basin, Spain. *Sedimentology*, **59(2)**, 356-378.

Olariu, C., **Steel, R.J., Vann, N., Tudor, E., Shin, M., Winter, R., Gan, Y., Jung, E., Almeida, F., Minisini, D., Brinkworth, W., Loss, L., Inigo, J.** and **Gutierrez, R.** (2019) Criteria for recognition of shelf-slope clinoforms using outcrop data; Jurassic Lajas and Los Molles formations, S. Neuquén Basin, Argentina. *Basin Research.* Online.

Paim, P. S., Silveira, A. S., Lavina, E. L., Faccini, U. F., Leanza, H. A., de Oliveira, J. T., and **D'Avila, R. S**. (2008) High resolution stratigraphy and gravity flow deposits in the Los Molles Formation (Cuyo Group, Jurassic) at La Jardinera region, Neuquén Basin. In *Revista de la Asociación Geológica Argentina. Simposio Jurásico de América del Sur*, **63(4)**, 728-753.

Paim, P. S. G., **Lavina, E. L. C., Faccini, U. F., Silveira, A.S., Leanza, H.,** and **D'Avila, R. S. F.** (2011) Fluvial-derived turbidites in the Los Molles Formation (Jurassic of the Neuquen Basin): Initiation, transport, and deposition, *In* Slatt, R. M., and Zavala, C. (eds.). Sediment transfer from shelf to deep water—Revisiting the delivery system: *AAPG Studies in Geology* **61**, p. 95–116.

Patruno, S., Hampson, G. J., Jackson, C. A. L., & **Dreyer, T.** (2015). Clinoform geometry, geomorphology, facies character and stratigraphic architecture of a sand-rich subaqueous delta: Jurassic Sognefjord Formation, offshore Norway. *Sedimentology*, **62(1)**, 350-388.

Patruno, S., & **Helland-Hansen, W.** (2018). Clinoforms and clinoform systems: Review and dynamic classification scheme for shorelines, subaqueous deltas, shelf edges and continental margins. *Earth-science reviews*, **185**, 202-233.

Paumard, V., Bourget, J., Payenberg, T., Ainsworth, B., Lang, S., Posamentier, H., & **George, A.** (2018). Shelf-margin architecture and shoreline processes at the shelf-edge: Controls on sediment partitioning and prediction of deep-water deposition style. *ASEG Extended Abstracts*, **2018(1)**, 1-6.

Peng, Y., Steel, R. J., and **Olariu, C.** (2017) Transition from storm wave-dominated outer shelf to gullied upper slope: The mid-Pliocene Orinoco shelf margin, South Trinidad. *Sedimentology*, **64(6)**, 1511-1539.

Perov, G., and **Bhattacharya, J. P.** (2011) Pleistocene shelf-margin delta: Intradeltaic deformation and sediment bypass, northern Gulf of Mexico. *AAPG bulletin*, **95(9)**, 1617-1641.

Petter, A. L., & **Steel, R. J.** (2006). Hyperpycnal flow variability and slope organization on an Eocene shelf margin, Central Basin, Spitsbergen. *AAPG bulletin*, **90(10)**, 1451-1472.

Plink-Björklund, P. and **Steel, R.J.** (2004) Initiation of turbidity currents: outcrop evidence for Eocene hyperpycnal flow turbidites. *Sed. Geol.,* **165,** 29-52.

Plink-Björklund, P. (2012) Effects of tides on deltaic deposition: Causes and responses. *Sedimentary Geology*, **279**, 107-133.

Porebski, S.J. and **Steel, R.J.** (2003) Shelf-margin deltas: their stratigraphic significance and relation to deepwater sands. *Earth-Sci.Rev.,* **62,** 283-326.

Postma, G., Nemec, W., & **Kleinspehn, K. L.** (1988). Large floating clasts in turbidites: a mechanism for their emplacement. *Sedimentary geology*, **58(1)**, 47-61.

Poyatos-Moré, M., Jones, G. D., Brunt, R. L., Hodgson, D. M., Wild, R. J., & **Flint, S. S.** (2016). Mud-dominated basin-margin progradation: processes and implications. *Journal of Sedimentary Research*, **86(8)**, 863-878.

Pyles, D.R., and **Slatt**, **R.M.** (2007) Applications to understanding shelf edge to base-of-slope changes in stratigraphic architecture of prograding basin margins: Stratigraphy of the Lewis Shale, Wyoming, USA. In *Atlas of deep-water outcrops* (Eds T.H. Nilsen, R.D. Shew, G.S. Steffens and J.R.J. Strudlick): *AAPG Studies in Geology,* **56**, CD-ROM, 1-19.

Ramos, V. (1999) Plate tectonic setting of the Andean Cordillera. *Episodes*, **22,** 183-190.

Reynaud, J.Y. and **Dalrymple, R.W.** (2011) Shallow-marine tidal deposits. In: Davis Jr., R.A., Dalrymple, R.W. (Eds.), Principles of Tidal Sedimentology. *Springer*, Dordrecht, pp. 335-369.

Ross, W.C., Watts, D.E. and **May, J.A.**, (1995) Insights from stratigraphic modeling: mud-limited versus sand-limited depositional systems. AAPG bulletin, **79(2)**, pp.231-258.

Rossi, V. M., and **Steel, R. J**. (2016) The role of tidal, wave and river currents in the evolution of mixed-energy deltas: Example from the Lajas Formation (Argentina). *Sedimentology*, **63(4)**, 824-864.

Ryan, M. C., Helland-Hansen, W., Johannessen, E. P., and **Steel, R. J.** (2009) Erosional vs. accretionary shelf margins: the influence of margin type on deepwater sedimentation: an example from the Porcupine Basin, offshore western Ireland. *Basin Research*, **21(5)**, 676-703.

Sassi, M. G., Hoitink, A. J. F., de Brye, B., & **Deleersnijder, E.** (2012). Downstream hydraulic geometry of a tidally influenced river delta. *Journal of Geophysical Research: Earth Surface*, **117(F4)**.

Schwartz, T. M., and **Graham, S. A**. (2015) Stratigraphic architecture of a tide-influenced shelf-edge delta, Upper Cretaceous Dorotea Formation, Magallanes-Austral Basin, Patagonia. *Sedimentology*, **62(4)**, 1039-1077

Silalahi, H. (2009) Stratigraphic architecture of slope deposits associated with prograding margins, Sobrarbe Formation: Ainsa Basin, Spain. Master's Thesis. Colorado School of Mines, Golden, CO. 146 pp.

Shanmugam, G. (1996). High-density turbidity currents; are they sandy debris flows?. *Journal of sedimentary research*, **66(1)**, 2-10.

Shchepetkina, A., **Gingras, M. K., Mángano, M. G.,** & **Buatois, L. A.** (2019). Fluvio-tidal transition zone: Terminology, sedimentological and ichnological characteristics, and significance. *Earth-science reviews*.

Souza, A. J., Alvarez, L. G., & **Dickey, T. D.** (2004). Tidally induced turbulence and suspended sediment. *Geophysical Research Letters*, *31*(20).

Steel, E., Simms, A.R., Steel, R. and **Olariu, C.** (2018) Hyperpycnal delivery of sand to the continental shelf: Insights from the Jurassic Lajas Formation, Neuquén Basin, Argentina. *Sedimentology*, **65(6)**, 2149-2170.

Steel, R. J., Crabaugh, J., Schellpeper, M., Mellere, D., Plink-Bjorklund, P., Deibert, J., and **Loeseth, T.** (2000) Deltas vs. rivers on the shelf edge: their relative contributions to the growth of shelf-margins and basin-floor fans (Barremian and Eocene, Spitsbergen). *Deepwater Reservoirs of the World*, **15(1)**, 981-1009.

Steel, R.J. and **Olsen, T.** (2002) Clinoforms, clinoform trajectories and deepwater sands. In: *Sequence Stratigraphic Models for Exploration and Production: Evolving Methodology, Emerging Models and Application Histories* (Eds J.M. Armentrout and N.C. Rosen), GCS-SEMP Found 22nd Annu Res Conf Proc, 367-381 (CD-ROM).

Steel, R. J., Olariu, C., Zhang, J. and Chen, S. (2019) What is the topset of a shelf prism?, *Basin Research Special Publications* (in press).

Stride, A. H. (1982) Offshore tidal deposits: sand sheet and sand bank facies. In *Offshore tidal sands* (pp. 95-125). Springer, Dordrecht.

Sydow, J., and **Roberts, H. H.** (1994) Stratigraphic framework of a late Pleistocene shelf-edge delta, northeast Gulf of Mexico. *AAPG bulletin*, **78(8)**, 1276-1312.

Sylvester, Z., Deptuck, M.E., Prather, B.E., Pirmez, C. and **O`Byrne, C.** (2012**)** Seismic stratigraphy of a shelf-edge delta and linked submarine channels in the northeastern Gulf of Mexico. *In*: Prather, B., Deptuck, M.E., Mohrig, C., Van Hoor, B. and Wynn, R.B, (eds.) Application of the principles of seismic geomorphology to continental-slope and base-of-slope systems: case studies from seafloor and near-seafloor analogues, *SEPM Society for Sedimentary Geology Special Publication,* **99**, 31-59.

Tooth, S., & **McCarthy, T. S.** (2004). Controls on the transition from meandering to straight channels in the wetlands of the Okavango Delta, Botswana. *Earth Surface Processes and Landforms: The Journal of the British Geomorphological Research Group*, **29(13)**, 1627-1649.

Uliana, M. A., Biddle, K. T., and **Cerdan, J.** (1989) Mesozoic Extension and the Formation of Argentine Sedimentary Basins: Chapter 39: Analogs. 599-614.

Uroza, C.A. and **Steel, R.J.** (2008) A highstand shelf-margin delta system from the Eocene of West Spitsbergen, Norway. *Sed. Geol.*, **203**, 229-245.

Vergani, G. D., Tankard, A. J., Belotti, H. J., and **Welsink, H. J.** (1995) Tectonic evolution and paleogeography of the Neuquén Basin, Argentina. *In*: Tankard, A.J., Suaréz Soruco, R. and Welsink, H.J. (eds) *Petroleum Basins of South America. AAPG Memoirs,* **62,** 383-402.

Vicente, J. C. (2005) Dynamic paleogeography of the Jurassic Andean Basin: pattern of transgression and localisation of main straits through the magmatic arc. *Revista de la Asociación Geológica Argentina*, **60(1)**, 221-250.

Zavala, C. (1996) Sequence stratigraphy in continental to marine transitions. An example from the Middle Jurassic Cuyo Group, south Neuquén Basin, Argentina. In *GeoResearch Forum* . **1(2)**, 285-293.

Zavala, C. (1996) High-resolution sequence stratigraphy in the Middle Jurassic Cuyo Group, South Neuquén Basin, Argentina. In *GeoResearch Forum*, **1(2)**, 295-303.

Zavala, C., and **Arcuri, M.** (2016) Intrabasinal and extrabasinal turbidites: Origin and distinctive characteristics. *Sedimentary Geology*, **337**, 36-54.

SEDIMENTOLOGY the journal of the International Association of Sedimentologists

Sedimentology (2020) doi: 10.1111/sed.12721

River-dominated and tide-influenced shelf-edge delta systems: Coarse-grained deltas straddling the Early–Middle Jurassic shelf–slope break and transforming downslope, Lajas–Los Molles formations, Neuquén Basin, Argentina

FLAVIO N. ALMEIDA JUNIOR*† , RONALD J. STEEL† , CORNEL OLARIU† , YUQIAN GAN† and PAULO S. GOMES PAIM*

**Programa de Pós-Graduação em Geologia, Universidade do Vale do Rio dos Sinos (Unisinos), Av. Unisinos, 950 - Cristo Rei, São Leopoldo - RS, 93022-750, Brazil (E-mail: flavionorbertoajr@gmail.com)*

†Jackson School of Geosciences, University of Texas at Austin, 2305 Speedway Stop C1160, Austin, TX 78712, USA

Associate Editor – Massimiliano Ghinassi

ABSTRACT

The three-dimensional facies and architecture variability of shelf-edge deltaic units cropping out at the transition between the Lower–Middle Jurassic Lajas and Los Molles formations of southern Neuquén Basin, Argentina, is presented here, as well as their stratigraphic relationship to uppermost deep-water slope channel systems. Deep-water, slope mudstones with thin turbidite beds merge upward with prodelta mudstones and thin sandstones, which are truncated by delta-front to mouth-bar sandstones. The latter sandstones are then downcut by large-scale, trough cross-stratified coarse-grained sandstones and conglomerates of distributary channel systems and alongstrike, amalgamated with cross-bedded sandy units showing evidence of tidal reworking. Proximal–distal facies and architecture variability within a shelf-edge deltaic succession demonstrates that distributary channel-complexes become wider and deeper basinward, forming channelized river-dominated distributary fairways separated by tidally reworked interdistributary sand belts at the shelf edge. Evidence from depositional-dip oriented outcrops shows a lack of collapsed and slumped strata at the shelf edge, and that the coarse shelf-edge distributary channel fills continue far down the deepwater slope, and conglomerates transform to become high-density turbidites to mainly thick-bedded, sand-matrix-supported debrites. The interplay between flood tides and river currents is interpreted to have primarily modulated the focusing of river drainages, and consequently coarse-grained sediment transport, along preferential routes on the outer-shelf to shelf-edge and down onto the slope. This contribution documents a unique example of coarse-grained (mostly conglomeratic) shelf-edge delta systems, tying bed-scale facies and architecture data to a seismic-scale shelf-margin morphology, thus providing outcrop analogue data for the characterization of shelf-edge delta systems in the subsurface.

Keywords Clinoform, Neuquén Basin, river-dominated, shelf-edge deltas, tide-influenced.

INTRODUCTION AND OBJECTIVES

Shelf-edge deltas occupy the morphologically defined topographic rollover area where the topset of a shelf margin passes basinward to a deepwater (>200 m depth) slope. Deltas at the shelf edge disperse significant volumes of sand to the slope and basin floor, both during sea-level lowstand (e.g. Mellere *et al.*, 2003; Johannessen & Steel, 2005; Sylvester *et al.*, 2012) or highstand (e.g. Carvajal & Steel, 2006; Covault *et al.*, 2007; Uroza & Steel, 2008). They are also usually the driver for basinward migration of the entire clinoform margin along this fairway (e.g. Sydow & Roberts, 1994; Steel *et al.*, 2000; Covault *et al.*, 2009; Dixon *et al.*, 2012a; Jones *et al.*, 2015), although progradation/accretion of shelf margin systems does not always imply deltas reaching the shelf edge (e.g. Hernández-Molina *et al.*, 2000; Reid & Patruno, 2015). In the latter cases, however, generally under flooded shelf conditions, shelf-edge deposits tend to be mud-prone because sand supply is scarce, and shelf-margin progradation occurs via dilute mud-rich gravity flows (e.g. Poyatos-Moré *et al.*, 2016). Shelf-edge deltas are therefore one of the fundamental building blocks of sand-prone progradational shelf-margins (Burgess & Hovius, 1998; Steckler *et al.*, 1999; Steel & Olsen, 2002; Porebski & Steel, 2003). The characterization of such systems elucidates the mechanisms and processes governing the dispersal of shelf-edge sand into deepwater areas of shelf margins, thus providing analogues for prediction of subsurface deepwater reservoir presence and de-risking of prospects (Johannessen & Steel, 2005).

Despite the importance of shelf-edge deltas, there is still a dearth of detailed sedimentological studies for such systems, sometimes due to the limited resolution of seismic data sets (Sylvester *et al.*, 2012) and because there is generally a limited number of shelf-edge deltaic systems exposed in uplifted orogenic belts. High-resolution sedimentological data provided the first examples of highly supplied highstand shelf-edge deltas, able to produce submarine fans (e.g. Carvajal & Steel, 2006; Covault *et al.*, 2007). It has also been shown that sediment delivery into deep water areas is likely also conditioned by process regime at the shelf-edge and may not work if deltas are not mainly fluvially driven (e.g. Dixon *et al.*, 2012b; Laugier & Plink-Björklund, 2016). Recent outcrop studies, however, are now providing substantial examples of how mixed-process (e.g. Gomis-Cartesio *et al.*, 2016) or storm wave-dominated shelf-edge deltas (e.g. Peng *et al.*, 2017) may also deliver considerable volumes of sand into deep-water areas.

The present study documents *ca* 300 m thick clinoforms cropping out in the Middle Jurassic Lajas and Los Molles formations (southern Neuquén Basin, Argentina). Mapping of distinct clinoform markers led to the identification of nine clinothems, seven of which exhibit an unusual assemblage of coarse-grained deposits (predominantly sandy-pebbly to conglomeratic) that prograded out onto pre-existing outermost shelf to upper slope mudstones. The aim of this work, using both depositional-dip and depositional-strike data, is to provide a three-dimensional, bed-scale facies and architectural model for coarse-grained shelf-edge deltas. How sediment moves from the shelf-break area of the margin, and how tidal currents play a role in this are also documented. This study describes a 'one of a kind' example of coarse-grained (mostly conglomeratic) shelf-edge deltas and its relationship to uppermost slope channel systems. In addition, how debris flows (cohesive and cohesionless) and turbidites are distributed across this shelf edge are also elucidated. This work builds further on previous research from Paim *et al.* (2008) and Olariu *et al.* (2019).

GEOLOGICAL BACKGROUND

The Neuquén Basin

Located on the eastern side of the Andes in western central Argentina and central Chile, between 31 and 41S latitude (Fig. 1A), the Neuquén Basin contains a near continuous, up to 4000 m thick, Late Triassic – Early Cenozoic sedimentary succession primarily controlled by the multi-episodic tectonic evolution of the western margin of Gondwana (e.g. Introcaso *et al.*, 1992; Vergani *et al.*, 1995; Ramos, 1999; Franzese *et al.*, 2003). Post-orogenic collapse (i.e. Gondwana Orogen) led to extension during Late Triassic – Early Jurassic, thus an initial rifting stage that produced a series of isolated depocentres infilled with non-marine strata of the Pre-Cuyo Group (Manceda & Figueroa, 1995; Vergani *et al.*, 1995; Franzese & Spalletti, 2001). Subsequent marine flooding into these basins during the Pliensbachian–Toarcian confined deposition within sub-basins in the southernmost parts of Neuquén Basin despite initiation of a steeply dipping subduction zone along the

western Gondwana margin, suggesting that rifting prevailed over subduction-induced thermal subsidence and effectively controlled sedimentation throughout the Early-Jurassic (Gulisano & Pando, 1981; Legarreta & Gulisano, 1989; Uliana *et al.*, 1989; Vergani *et al.*, 1995; Burgess *et al.*, 2000).

By mid-Jurassic times the rift-phase is thought to have been replaced by a more laterally extensive post-rift stage due to back-arc thermomechanical extension (Vergani *et al.*, 1995; Legarreta & Uliana, 1991; 1996). Recent studies in southernmost Neuquén Basin (Kim *et al.*, 2014) have demonstrated, however, that differential subsidence between blocks and depocentres in the Bajocian sub-basins was still very active in parts of this southernmost area. The post-rift back-arc stage remained active until Early Cretaceous, and saw growth of a shelf system dominated by a series of transgressive–regressive cycles representative of middle and upper Cuyo, Lotena and Mendoza groups (Vergani *et al.*, 1995). A decreasing angle of slab subduction at the end of the Early Cretaceous led to tectonic compression that caused Late Cretaceous Andean uplift and development of a foreland stage that characterizes the modern Neuquén Basin (e.g. Vergani *et al.*, 1995; Franzese *et al.*, 2003).

Early to Middle Jurassic Cuyo Group stratigraphy

The present study is in the Lower to Middle Jurassic Cuyo Group succession, particularly the transition between the muddy Los Molles Formation and the sand-rich Lajas Formation, in the southernmost reaches of the basin (Fig. 1A and B). The marine mudstones of the Los Molles Formation represent relatively deep water (>300 m) conditions dominated by sediment gravity flows with thick turbidite deposits in places (Zavala, 1996a,b; Burgess *et al.*, 2000; Howell *et al.*, 2005; Paim *et al.*, 2008). The Lajas Formation, on other hand, represents shallow-water neritic conditions, a shelf rimming the deepwater area, dominated by deltas, distributary channels and estuaries (e.g. Gulisano *et al.*, 1984; Legarreta & Uliana, 1996; Zavala, 1996a,b; McIlroy *et al.*, 2005; Paim *et al.*, 2008, 2011; Gugliotta *et al.*, 2015; Rossi & Steel, 2016).

Lajas and Los Molles formations were traditionally seen as distinct tabular stratigraphic units essentially separated from one another and from the overlying fluvial deposits (Challaco Formation) by erosive discordance surfaces (e.g. Zavala, 1993; Veiga, 2000; Zavala & González, 2001). However, as in most deepwater sedimentary basins, seismic data now show that such a 'layer-cake' model is unlikely, and that the lithostratigraphic formations are diachronous and partly proximal–distal equivalents with one another (e.g. Brinkworth *et al.*, 2017). Already by the mid-1980s (Gulisano *et al.*, 1984) the clinoformal configuration of Jurassic stratigraphy had been proposed, representing one of the earliest understandings that the Los Molles, Lajas and Challaco formations could be coeval units and laterally equivalent to each other as topset–foreset and toeset clinoform strata. Paim *et al.* (2008) mapped timelines/clinoforms up through the Los Molles Formation, but did not continue the timelines through the Lajas and Challaco formations. The breakthrough came with recent seismic data (e.g. Brinkworth *et al.*, 2017), which showed that the Cuyo Group consists of a series of progressively prograding clastic wedges (albeit with several internal discontinuities, for example intra-Bajocian unconformity) where all wedges consist of fluvio-marine topset, deepwater slope and submarine fan bottomsets (Fig. 1C).

In the present study area, around Arroyo La Jardinera (Figs 1A and 2), southernmost Neuquén Basin, Argentina, there is near stratigraphic continuity between the older, deepwater basin-floor and slope mudstones and the shallow-water shelf deposits, and in places clinoform marker horizons have been identified (yellow arrows, Fig. 2B), showing that the sandy Lajas shelf deposits penetrate distally down into the deepwater mudstones of the Los Molles Formation, and transit landward to the coeval fluvial system of the Challaco Formation (Olariu *et al.*, 2019). The significance of such clinoformal patterns is that they allow the position of the shelf edge or the shelf–slope break to be exactly pinpointed in the stratigraphy, and mapped across the area. Although previous studies have recognized diachronous boundaries between the Los Molles and Lajas formations (e.g. Gulisano *et al.*, 1984; Zavala, 1996a,b), the character of the linkage between shallow-water shelf and the deepwater turbidite depositional systems has rarely been addressed.

STUDIED OUTCROPS: ARROYO LA JARDINERA AREA

In the studied area of Arroyo La Jardinera, kilometre-long outcrop belts continuously expose alluvial and shallow-marine shelf deposits together

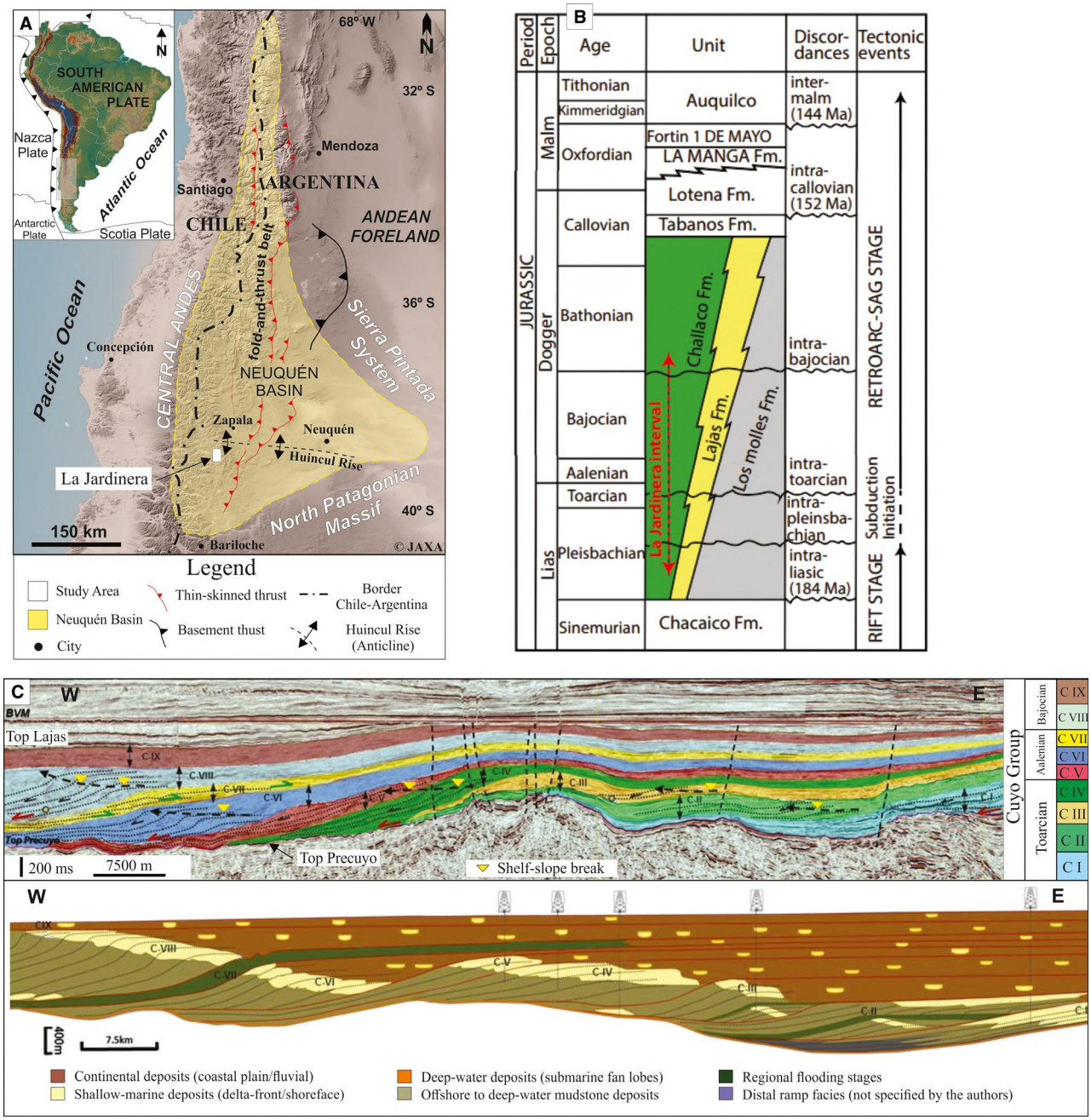

Fig. 1. (A) Location map of the Neuquén Basin in South America, indicating the main localities and the studied area of La Jardinera. (B) Stratigraphic chart of southern Neuquén Basin (from Olariu *et al.*, 2019; after Vergani *et al.*, 1995; Riccardi *et al.*, 2000; Paim *et al.*, 2008; Kochhann *et al.*, 2011). (C) West–east seismic cross-section along southern Neuquén Basin followed by interpretation. Note that the seismic data shows clearly that the Cuyo Group consists of a series of progressively prograding clastic wedges, where all wedges consist of fluvio-marine topset, deepwater slope and submarine fan bottomsets (i.e. clinoform geometries). Note that landward transgressions in Lajas are quite modest maximum *ca* 10 km, likely reflecting greenhouse (low amplitude) eustatic changes (modified from Brinkworth *et al.*, 2017).

with slope and basin floor deposits (Paim *et al.*, 2008) (Fig. 2A and B). They represent diachronous lithostratigraphic units that are laterally equivalent to one another as top sets (Challacó and Lajas formations) and deep-water deposits (Los Molles Formation) arranged into (at least) four sets of *ca* 250 m thick shelf-margin clinoform systems (fig. 5 in Olariu *et al.*, 2019) (Fig. 2C). Single topset

sequences on the shelf consist of an upward coarsening regressive unit (often with several internal parasequences) followed by an upward fining, transgressive unit (Olariu *et al.*, 2019; Steel *et al.*, 2019). These phases represent the regressive transit of deltas across the shelf followed by transgressive backstepping of the same deltas, leading to clinoform buildout (Ross *et al.*, 1995; Carvajal & Steel, 2006). Repeated sequences of this type stack on top of one another. The boundaries between sequences are taken as the finest grained intervals (maximum flooding surfaces) at the turnaround from transgression to regression (method of Galloway, 1998).

This work focuses on the critical *ca* 60 m thick strata of the Late Toarcian to Aalenian–Bajocian clinothem rollovers, along two long cross-sections capturing the Lajas–Molles transition, where unusually thick, upward-coarsening deltaic successions occur right above slope mudstones. Note that Lajas and Los Molles transition strata (in the La Jardinera area, but not throughout the whole Lajas stratigraphy) represent shelf–slope break deposits, and that here in the Neuquén Basin, as elsewhere, the Lajas topset at the shelf edge area tends to thicken (compared to coeval mid or inner-shelf Lajas deposits) as an outermost-shelf sandstone belt (see also Porebski & Steel, 2003). One studied cross-section is *ca* 5 km long, nearly depositional-strike oriented (see palaeocurrent map, Fig. 2A) and contains the Don Cordero shelf-edge delta deposits dated to Aalenian or earliest Bajocian (Kochhann *et al.*, 2011). The second cross-section, adjacent to the first but slightly older, is *ca* 4 km long, nearly depositional-dip oriented and contains the conglomeratic Bey Malec shelf-edge delta deposits that can be seen to form long downslope (clinoformal) coarse-grained 'timelines' that penetrate far down into the deepwater slope of the Los Molles Formation. The Bey Malec system lies immediately above a volcanic ash horizon dated to Late Toarcian, i.e. deposits most likely to be earliest Aalenian (Daniel Minisini, pers. comm.)

STRATIGRAPHIC METHODS

Data collection

Centimetre to decimetre-scale sedimentological data have been measured through *ca* 2100 m of outcrop in sections oriented both along depositional strike (Don Cordero section) and near-depositional dip (Bey Malec section), thus providing a two-dimensional and three-dimensional control of facies variability across the shelf edge zone in an area of 10×20 km (Fig. 2A). A total of 258 palaeocurrent readings have been measured from cross-strata, current ripple lamination, channel axes, sole marks and clast imbrication. Palaeocurrent directions were restored to their pre-tectonic tilt attitude. Lithostratigraphic logs were coupled with drone 'photopanels', a high-resolution digital elevation model (DEM) and hundreds of georeferenced points of control acquired by walking along the main stratigraphic boundaries. Thus, an accurate correlation of the major process-sedimentology boundaries and a multi-scale architectural reconstruction of the shelf-edge deposits was obtained.

How was the shelf edge identified in the stratigraphy?

Basins are usually required to have at least 200 m of water depth to develop a shelf-margin clinoform (Steel & Olsen, 2002), so that water depth (bathyal) exceeds that found on most shelves. Sedimentary wedges that build out from the margin of such basins often exhibit large-scale (hundreds of metres), topset–foreset clinoform geometries (e.g. Johannessen & Steel, 2005; Pyles & Slatt, 2007; Houseknecht *et al.*, 2009; Hubbard *et al.*, 2010; Gomis-Cartesio *et al.*, 2018; Patruno & Helland-Hansen, 2018). Deepwater basins therefore have a shelf-margin morphology of flat to gently sloping shelf, together with a steeper deepwater slope (commonly 1 to 4°), and a gently sloping to flat basin floor. The two inflection points along the margin morphology are the shelf–slope break, and the toe-of-slope break. In seismic data the rollover of the shelf–slope break is generally obvious, in outcrops, however, it is less easy to identify. The present study focuses on both the imaged morphological rollover and the threshold between shallow-water, neritic facies, dominated by waves or by river and tidal currents, and the deepwater slope facies where sediment gravity flows dominate.

Shelf-edge deltas, by definition, occupy the outermost part of the topset or shelf and straddle the shelf–slope break. The identification of large-scale clinoform bounding surfaces not only allows the zone of shelf–slope break to be pinpointed in the stratigraphy, but also enables a correlation between shelf and upper-slope deposits as coeval systems. It should be noted that the

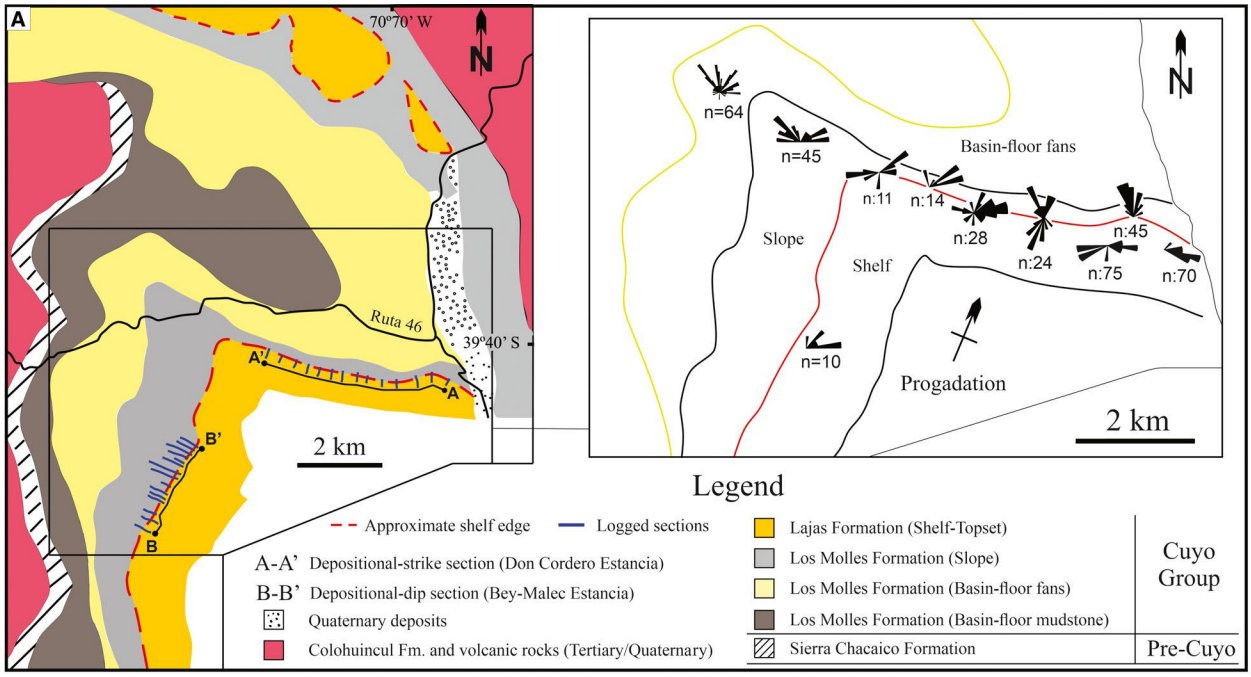

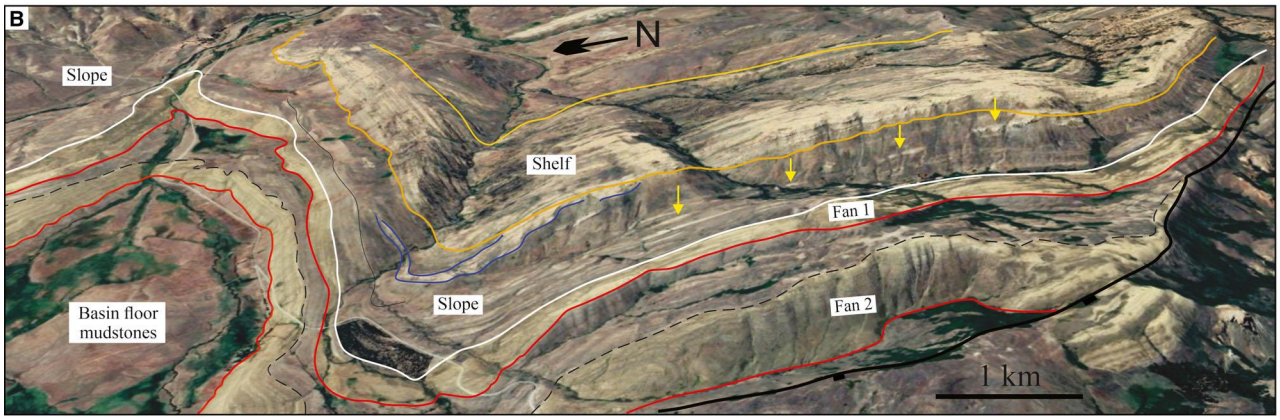

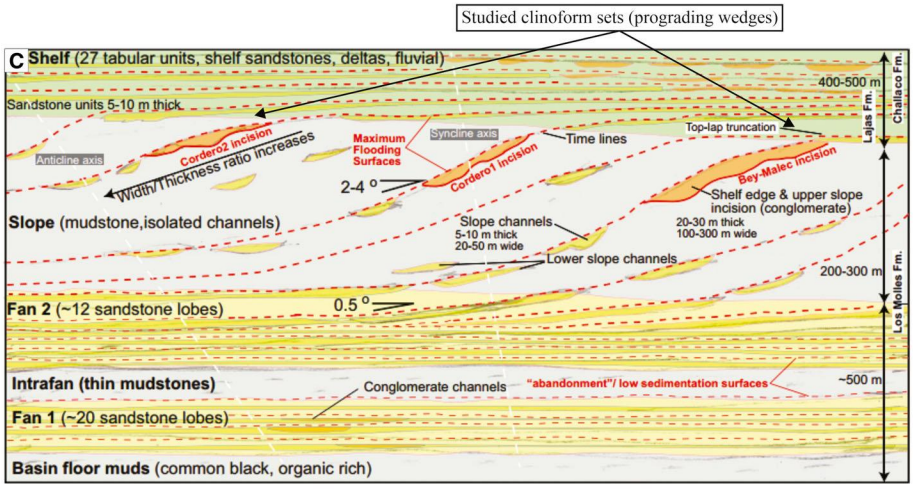

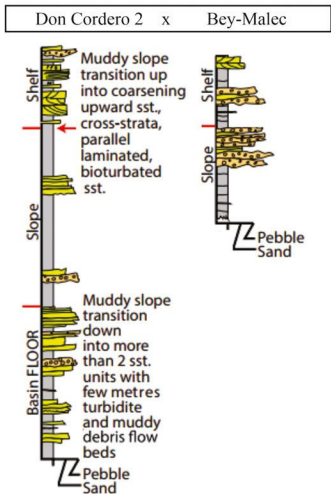

Fig. 2. (A) Geological map of La Jardinera area (after Paim *et al.*, 2008; Olariu *et al.*, 2019) showing the strike and dip cross-sectional profiles where sedimentary data have been acquired, i.e. A–A' Don Cordero and B–B' Bey Malec, respectively (logged sedimentary sections represented by blue lines). Palaeocurrent measurements are displayed on an attached map and indicate shelf-margin system progradation towards the north-east. (B) Birds eye view of southern of La Jardinera area (satellite image) showing the tripartite of the shelf-margin depositional environments (i.e. sandy shelf – muddy slope – sandy basin-floor fans). Note the lowermost light coloured sandstone benches within the dark coloured (green) Los Molles mudstones can be seen to rise stratigraphically upward to the right, towards the overlying Lajas sandstones (yellow arrows) (see Fig. 3 for better visualization). This is a tongue of Lajas sandstones that penetrated down into the coeval muddy Los Molles Formation. (C) Clinoform stratigraphy model proposed by Olariu *et al.* (2019), where (at least) four shelf-margin clinoform sets (prograding wedges) are interpreted. Generalized stratigraphic sections for the Lajas–Molles transition in the two studied outcrop belts are also included (modified from Olariu *et al.*, 2019).

shelf break occurs in two different stratigraphic settings. In one scenario where successive clinothems prograde but also aggradationally stack on each other (sigmoidal clinoforms), the topset of any clinothem passes gradually into the slope segment of the same clinoform; in the second scenario, where the topset is more strongly progradational and shows channelized down-cutting (oblique clinoforms), there is a clear erosive unconformity developed between topset and slope (e.g. Mitchum *et al.*, 1977; Ryan *et al.*, 2009), although the approximate position of the migrating shelf break can still be gleaned. The latter is commonly developed where topset progradation is forced by relative sea-level fall (Mitchum *et al.*, 1977). In addition to imaging the clinoform rollover as above and lithology changes from wave, tide and river-generated facies to dominantly sediment gravity flows (Dixon *et al.*, 2012a), it is sometimes possible to confirm the shelf break by monitoring an increasing degree of slope instability, seen by large-scale soft-sediment deformation (Plink-Bjorklund & Steel, 2005, fig. 21).

How were the Lajas–Los Molles clinoforms reconstructed in the outcrops?

Clinoform geometries were reconstructed and stratigraphic sequences were defined in the outcrops by two methods. The first, and most commonly used method (e.g. Steel & Olsen, 2002), involves mapping the repeated, key flooding surfaces in the shelf stratigraphy, i.e. muddy intervals below regressive and above transgressive deposits. These muddy intervals in the topset deposits are normally widespread but thin (5 to 10 m) and sometimes directly overlie shell and conglomeratic transgressive lag deposits. Further, they can be mapped in their downslope continuation (abandonment surfaces) into deepwater deposits. The second method deviates from the above 'textbook' method, and involves mapping coarse-grained channel fills on the shelf that penetrate continuously or discontinuously (but closed spaced) across the shelf break and continue downslope as a correlative coarse-grained timeline within the muddy slope (Fig. 3). The slope inclination can be seen with respect to a palaeo-horizontal datum (e.g. Magallanes Basin, Hubbard *et al.*, 2010) and sometimes these coarse incursions in the slope provide optimal imaging of the gradient. In the present study, an adjacent topset flooding surface in the overlying shelf stratigraphy was chosen as a local datum since it represents a quasi-horizontal surface when projected landward (Fig. 3B).

SEDIMENTOLOGICAL RESULTS AND INTERPRETATIONS

Twenty-four facies (F) have been distinguished (Table 1). Six facies associations (FA) have then been defined by grouping of spatially related and genetically coherent facies, both in terms of vertical and lateral transitions, and their position along the physiographic shelf-margin profile. Facies association characteristics are summarized in Table 2, and some of the more detailed sedimentological and architectural aspects of FA are further described below within the context of depositional elements of shelf-edge deltaic systems.

Shelf-edge delta lithofacies succession

In both studied outcrop belts, i.e. along depositional dip-oriented and strike-oriented cross-sections, shelf-edge deltaic successions consist of up to 70 m thick, stacked upward-coarsening facies successions or parasequences that directly overlie >250 m deep-water mudstones with

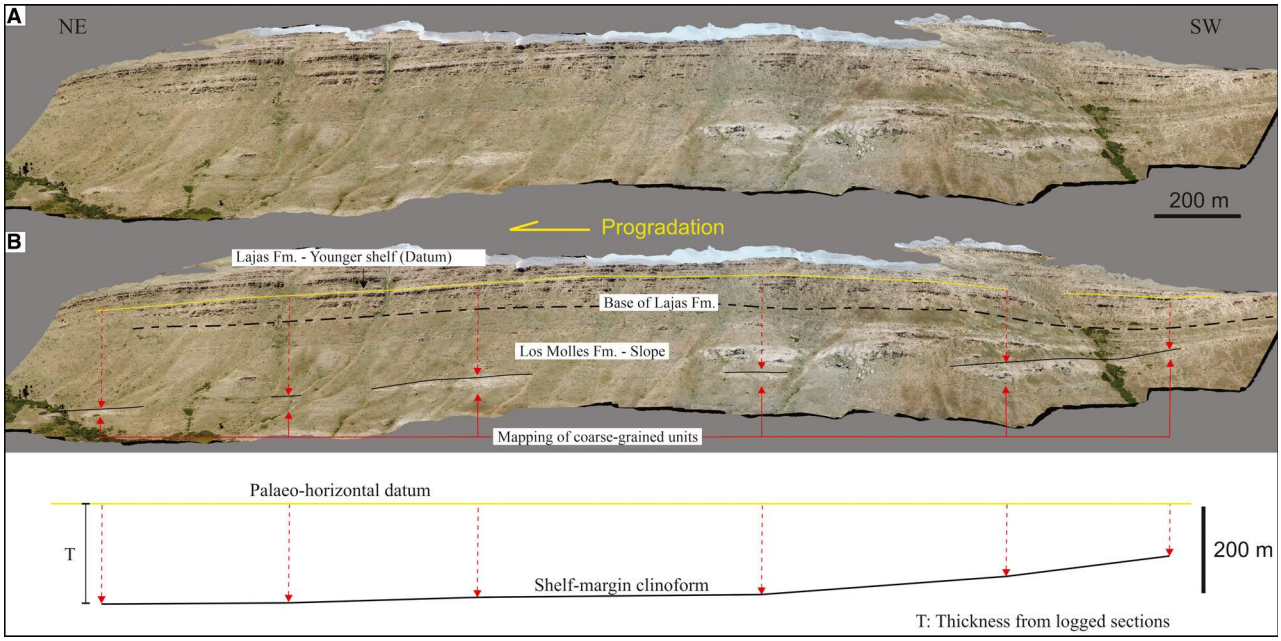

Fig. 3. Reconstruction of the Lajas–Molles clinoform stratigraphy in outcrops. (A) Composite drone photographic panel along depositional-dip cross-section (Bey Malec Estancia). (B) Reconstruction of clinoform stratigraphy consisted of mapping the coarse-grained channel fills on the shelf that penetrate across the shelf break and continue downslope as correlative coarse-grained units within the muddy slope. The slope inclination can be seen with respect to a palaeo-horizontal datum, i.e. an adjacent topset flooding surface in the overlying shelf stratigraphy was chosen as a local datum since it represents a quasi-horizontal surface when projected landward. It is important to note that, even though slope inclination can be seen from measured stratigraphic thicknesses and photomosaics, it is underestimated, because decompaction has not been applied.

thick sediment gravity flow deposits in places (see type-log, Fig. 4). Each upward-coarsening facies succession within the *ca* 70 m thick shelf-edge delta interval changes upward from thin conglomeratic or shell lags (Fig. 4A) and marine mudstones to prodelta mudstones with thin sandstones (FA2), low-angle laminated delta-front to mouth-bar sandstones (FA3) and are then downcut by large-scale, trough cross-stratified coarse-grained sandstones and conglomerates of distributary channel systems (FA4). The entire shelf-edge delta succession is then overlain by tens of metres thick transgressive marine mudstones with embedded sandstones.

The boundary between the hundreds of metres thick slope mudstones embedding thin turbidites and the overlying prodelta mudstones with thin sandstones (Fig. 4B) is relatively difficult to pick. However, the boundary is set along the zone of marked increase in: (i) sandstone/mudstone ratio, as well as presence of an upward-coarsening depositional trend (Fig. 4C); (ii) bioturbation; predominantly occurrences of vertical burrows (*Skolithos*) (Fig. 4D); and (iii) organic plant debris. Note that the term 'slope' is used here exclusively for the physiographically defined slope (Los Molles Formation). Prodelta mudstones and thin sandstones, on the other hand, are distal deltaic units deposited on the outer-shelf to uppermost slope as expected for a shelf-edge deltaic succession (see interpretation in Table 2, i.e. Lajas Formation).

Prodelta and lower delta-front deposits occur as an 8 to 25 m thick interval of upward coarsening and thickening, fine to coarse-grained sandstones alternating with some thin-laminated mudstones. Sandstone units contain abundant plant debris and mud rip-up clasts, and exhibit soft-sediment deformation (F13) or contain collapsed intraformational blocks in places (F12) (Fig. 4E). Storm-wave sedimentary structures, such as hummocky and swaley cross-stratification, are all but absent. Prodelta and lower delta-front deposits are overlain sharply by upward-coarsening and thickening, flat to low-angle stratified (F17), medium-grained to conglomeratic sandstone units interpreted as distributary mouth-bar deposits (Fig. 4F). These sandstone bodies are not channelized but are sheet-like, up to 10 m thick, with composite metre-scale, well-laminated bedsets that stack and

Table 1. Lithofacies descriptions and interpretations.

Name	Code	Thickness	Boundaries	Texture	Sedimentary structures	Depositional processes
Mudstone	F1	Centimetre to hundreds of metres thick	Gradational to sharp, non-erosive bases (lithological boundary); sharp or gradational upper boundaries.	Silt-rich mudstones with lenses of very-fine sandstone	Fissility (i.e. shales)	Pelagic and hemipelagic mud settled by suspension fallout in slack-water conditions or/and fluid mud deposition by turbulent (low-density) to non-turbulent flows
Centimetre-bedded, non-laminated to laminated mudstones and sandstones	F2	Centimetre to tens of metres thick	Gradational to sharp, non-erosive bases (lithological boundary)	Silt-rich mudstones alternated with very-fine to fine sandstones	Thin planar-parallel lamination to cross-lamination or grading, but mostly structureless	Alternating deposition between: (i) pelagic and hemipelagic mud settled by suspension fallout in slack-water conditions or/and fluid mud deposition by turbulent (low-density) to non-turbulent flows; and (ii) deposition by 'surge-type', sandy low-density turbidity currents (Bouma, 1962; Lowe, 1982)
Non-graded to normal graded and laminated sandstones	F3	Beds: 0.1–0.4 m thick; bedsets <1.5 m thick	Slightly irregular, sharp to non-erosive bases; Sharp to gradational upper boundaries	Medium to lower coarse-grained sandstones; well-sorted	Planar-parallel lamination, with or without normal grading	Deposition by 'surge-type', sandy low-density turbidity currents (*sensu* Lowe, 1982), equivalent to 'Bouma b' (*sensu* Bouma, 1962)
Structureless to graded sandstones with floating pebbles	F4	Beds: 0.2–1.5 m; up to 4 m thick bedsets	Sharp erosive bases and sharp (both lithological and erosional) upper boundaries	Upper medium to conglomeratic sandstones with <10% of isolated pebbles (MPS: 3 cm)	Normal grading, otherwise structureless	Deposition by high-density turbidity currents (*sensu* Lowe, 1982)
Sandstones with traction carpets	F5	Beds: 0.5–1.5 m thick; packages are up to 5 m thick	Irregular sharp erosive bases; sharp to gradational upper boundaries	From coarse-grained to conglomeratic sandstones; moderately sorted (MPS: 3 cm)	Normal grading, but predominantly structureless	Deposition by high-density turbidity currents (*sensu* Lowe, 1982)

Table 1. (continued)

Name	Code	Thickness	Boundaries	Texture	Sedimentary structures	Depositional processes
Mud clast-rich, non-graded to graded sandstones	F6	Beds: up to 0.4 m thick	Sharp erosive bases, and sharp (both lithological and erosional) upper boundaries	Medium to conglomeratic sandstones with variable degrees of sorting (from well to poorly-sorted sediments)	Inverse to normal grading, but predominantly structureless	Deposition by current suspended sediment flows that incorporated mud pieces by eroding underlying mudstone substrates
Non-graded to graded and poorly-sorted, sand-matrix-supported conglomerates	F7	Beds: 0.5–2.0 m thick; tens of metres composite units	Sharp erosive boundaries	Poorly-sorted, sand-matrix-supported conglomerates	Inverse to normal grading, otherwise structureless	Deposition by cohesive to mostly non-cohesive (cohesionless) debris flows
Non-graded to graded and poorly-sorted, clast-supported conglomerates	F8	Beds are up to 0.6 m thick	Sharp erosive boundaries	Poorly-sorted, clast-supported conglomerates with less than 20% of coarse to very coarse-grained sand matrix	Normal grading, but predominantly structureless	Deposition by hyperconcentrated to non-cohesive debris flows
Structureless sandstone	F9	Beds are <1 m thick	Irregular sharp erosive to non-erosive bases; sharp to gradational upper boundaries	Very fine to conglomeratic sandstones	Structureless	Deposition by turbulent flows in which near-bed turbulence and traction become suppressed (Arnott & Hand, 1989) or by turbulent flows with high near-bed sediment concentrations that are subject to hydraulic jump (Postma *et al.*, 2009)
Scour and fill cross-stratified sandstone	F10	Up to 0.6 m thick	Sharp erosive boundaries	Medium-grained sandstones to conglomerates	Isolated concave-up based cross-bedding	Deposition by the infilling of erosional scours

Table 1. (continued)

Name	Code	Thickness	Boundaries	Texture	Sedimentary structures	Depositional processes
Aggradational wave-rippled sandstone	F11	Beds are up to 0.3 m thick	Non-erosive bases; sharp to gradational upper boundaries	Fine to medium-grained sandstones	Strongly aggradational stacking of symmetrical ripples, which can infrequently display normal grading	Deposition by sustained (quasi-steady flow) turbidity currents, possibly river-generated hyperpycnal flows influenced by storms below the fair weather base
Slumped-collapsed blocks	F12	<1 m thick	Sharp erosive to discordant contacts	From medium-grained sandstones to conglomerates	Collapsed blocks allocated into underlying (commonly finer grained) rocks	Local deformation resulted from coherent mass-movements
Soft-deformed sandstones	F13	<0.4 m thick	Sharp boundaries (discordant at times)	Fine-grained sandstones	Convoluted bedding with flame structures	Resulted from fluidization and liquefaction of unconsolidated sediments in water-saturated environments
Storm-wave beds	F14	Beds are up to 0.3 m thick	Irregular sharp erosive to non-erosive bases; sharp to gradational upper boundaries	From fine to upper medium-grained sandstones	Hummocky and wave-ripple cross-lamination	Reworking and remobilization of unconsolidated sediments by the action of waves and storms below the fair weather base
Current ripple laminated sandstones	F15	Beds are up to 0.2 m thick	Sharp lithological to gradational contacts	Fine to medium-grained sandstones	Asymmetrical ripples with cross-lamination	Sand beds deposited or modified by unidirectional currents under lower flow regime
Flat-laminated sandstones with normal and inverse lamina-set grading	F16	Beds are up to 1 m thick; up to 15 m composite bedsets	Irregular sharp erosive erosive bases; sharp to gradational upper boundaries	Fine-grained to predominantly medium to lower coarse-grained sandstones	Planar parallel to low-angle lamination (characteristically thick lamina), with normal and inverse lamina-set grading	Deposition by sustained (quasi-steady flow) turbidity currents, possibly river-generated hyperpycnal flows
Non-graded, flat to low-angle stratified sandstones	F17	Beds are 0.4–1.0 m thick; bedsets are up to 2 m thick; <10 m composite bedsets	Sharp boundaries (slightly discordant and erosive at times)	Medium-grained to conglomeratic sandstones	Planar parallel to low-angle stratification	Upper stage plane-bed transport (upper flow regime) by strong unidirectional currents with high suspension load

Table 1. (continued)

Name	Code	Thickness	Boundaries	Texture	Sedimentary structures	Depositional processes
Planar cross-stratified sandstones	F18	0.2–0.6 m thick, cross-bed sets	Non-erosive to erosive bases; sharp (both lithological and erosional) upper boundaries	Medium to coarse-grained sandstones	Planar cross-stratification. Herringbone cross-beds and reactivation surfaces are recurrent	Migration of dune bedforms by both unidirectional currents, and reversing (tidal) currents
Planar cross-stratified sandstones with foreset mud – organic-draped bundles	F19	0.2–0.6 m thick, cross-bed sets	Non-erosive to erosive bases; sharp (both lithological and erosional) upper boundaries	Medium-grained sandstones, characteristically well-sorted	Planar cross-stratification with recurrent herringbone cross-beds with foreset mud or organic-draped bundles. Reactivation surfaces are common	Deposition by reversing (tidal) currents
Sandstone sets with small-scale trough cross-stratification	F20	0.1–0.3 m thick, cross-bed sets	Sharp erosive boundaries	Medium-grained sandstones, characteristically well-sorted	Trough cross-stratification	Migration of dune bedforms by unidirectional currents
Trough cross-stratified, conglomerates and pebbly sandstones	F21	Up to 1.5 m thick cross-bed sets, to tens of metres cosets	Sharp erosive boundaries	Pebbly-sandstones to conglomerates. MPS ranges from 1–10 cm	Trough cross-stratification	Migration of dune bedforms in high-energy stream flows
Non-graded to graded and moderately-sorted, clast-supported conglomerates	F22	Beds: up to 1.5 m thick; bedsets up to 3 m thick	Sharp erosive boundaries	Moderately-sorted conglomerates. MPS ranges from 1–10 cm	Structureless or normal grading	Bedload gravel deposited in stream flows during higher discharges
Shell-beds	F23	<0.4 m thick	Sharp erosive bases, and sharp (both lithological and erosional) upper boundaries	Shell fragments are commonly associated with well-sorted fine to medium-grained sandstones	Structureless, with shell fragments chaotically distributed within beds	Condensed skeletal concentrations resulted from deepening (transgression) of the palaeo-shoreline.
Organic detritus-rich sandstones	F24	<1 m thick	Sharp boundaries	From medium-grained to pebbly sandstones, typically poorly-sorted	Structureless, with charcoal detritus and large amounts of mud rip-up clasts	Accumulation resulted from organic detritus motion over sand and conglomeratic stream beds

Table 2. Summary of descriptions and interpretations of facies associations (FA).

Facies Association (FA)	Facies	Description	Interpretation
Facies Association 1 (FA1): Mudstone to thin-bedded mudstone and sandstones	F1, F2, F3	Metre-thick to tens of metres thick mudstone intervals normally containing thin sandstone lenses. Packages are predominantly thin-bedded siltstone and sandstones, often with higher amounts of organic detritus. Bioturbation incipient	Thick mudstone deposits result from hemipelagic suspension fallout in slack-water conditions and from fluid mud deposition by turbulent to non-turbulent flows *on the shelf or deepwater settings* (Harms *et al.*, 1982; Stow & Piper, 1984). The graded and laminated beds reflect deposition by sand-rich, low-density turbidity currents (Bouma, 1962)
Facies Association 2 (FA2): Medium bedded, amalgamated sandstones interbedded with thin-bedded sandstones–mudstones	F1, F2, F3, F4, F5, F9, F11, F12, F13, F14, F15	10–25 m thick intervals of upward coarsening and thickening, fine to coarse-grained sandstones alternating with some mudstones that directly overlie >250 m thick marine slope mudstones. Within these thick units an upward increase in sand–mud ratios corresponds with a higher degree of sandstone amalgamation, characterizing these deposits as having a lower muddy and upper sand-rich portions. The lower mudstones (up to 18 m thick) show an upward transition of increasing silt percent from the underlying (>250 m thick) slope mudstones. They consist of up to 1 m thick mudstones (F1) and thin-bedded, non-laminated to laminated mudstones and sandstones (F2) alternating with 0.1–0.2 m sandstone beds forming bedsets up to 0.5 m thick. Sandstone beds are fine to medium-grained, tabular, sharp-based and characteristically structureless (F9), or in some cases, non-graded to normal graded and laminated (F3). The upper sandy portions of the thick units are up to 7 m thick. They are characterized by up to 2 m thick, sandstone bedsets alternating with, up to 0.3 m thick non-laminated to laminated mudstones and sandstones. The sandstone bedsets form irregularly erosive, sharp-based sheets, range from medium to coarse-grained, and are relatively well-sorted	The characteristic upward coarsening of these interbedded units is interpreted to indicate basinward progradation of *prodelta* (*lower muddy units*) *and lower delta-front* (*upper sand-rich units*) *sedimentary environments* deposited on outermost-shelf to upper-slope settings
Facies Association 3 (FA3): Stacked co-sets of medium- to thick-bedded, flat to low-angle stratified sandstones	F10, F17	Upward coarsening and thickening, flat to low-angle stratified upper medium-grained to conglomeratic sandstone units. These sandstone bodies constitute non-channelized amalgamated bedsets that are up to 2 m thick that usually display forward accretion stacking patterns, indicated by metre-scale internal dipping (towards N-NE), carbonaceous material-draped clinoform	The overall upward-coarsening character of deposits and their association with channelized conglomerates (both large-scale and small-scale channel systems) are interpreted to represent distributary mouth-bar deposits. The lack of evidence for subaerial exposure suggests that these

Table 2. (continued)

Facies Association (FA)	Facies	Description	Interpretation
		surfaces. Individual beds range from 0.4–1.0 m thick, have slightly erosive sharp bases. Up to 30 cm thick, scour and fill cross beds occur isolated within bedsets. These sand units commonly associate with channelized conglomerates	are *subaqueous distributary mouth-bars and are part of the upper delta-front system*
Facies Association 4 (FA4): Channelized, cross-stratified sandstone and conglomerate units	F9, F21, F22	FA4 is composed of channelized and erosively based, trough cross-stratified (large-scale, >1 m thick) or occasionally structureless, clast-supported conglomerates interdigitated with coarse-grained to pebbly sandstones (up to 5 m thick and tens of metres in width). Displays widespread basal erosion surfaces that show an increased basal grain size and the presence of large amounts of mud rip-up clasts and organic detritus. MPS (maximum particle size) of 12 cm. These channelized units are closely associated with mouth-bar deposits (FA3)	The incision of the coarse-grained channels into mouth bar to delta front and prodelta deposits suggests that these channel-fills represent *lower delta-plain distributary-channel systems*
Facies Association 5 (FA5): Stacked co-sets of medium-bedded, thickly-laminated and well-sorted sandstones	F10, F16	Homogeneous, sharp-based and well-sorted (containing no conglomerate clasts) fine to predominantly (>70%) medium to lower coarse-grained, flat-laminated sandstone units (F15) up to 3 m thick, with beds up to 1 m thick. Although sand bodies are primarily pervasively flat-laminated (commonly very thick or 'spaced' lamination), they may also exhibit scattered centimetre-scale, shear-induced bedding deformation and occasional scour and fill cross-beds (F10). Normal–inverse lamina set grading. The composite bedsets are non-channelized sand bodies with relatively flat lower-bounding surfaces	*Hyperpycnite sand-lobes deposited on the outermost shelf*. Interpretation of sandy hyperpycnal shelf lobes suggest locations where gravelly dispersal did not reach the shelf edge or where the sandy shelf lobes were simply forerunners of the over-riding gravelly deltas
Facies Association 6 (FA6): Orderly stacked, planar to trough cross-stratified sandstone sets	F18, F19, F20	Orderly stacked sets of planar and some trough cross-strata, commonly truncated by reactivation surfaces, and show few mud drapes but some have a configuration of climbing compound dunes. They also contain marine fossils and trace fossils	Tidal reworking of sands occurring on the shelf, in tide-dominated deltas or in estuary mouths (e.g. Stride, 1982; Dalrymple & Rhodes, 1995; Olariu *et al.*, 2012a,b)

The italic aims to highlight the interpretation of depositional systems from facies associations description.

dip gently towards the NNE (regional downslope) (Fig. 4G). They also contain some carbonaceous laminae (Fig. 4H). These sandstones are infrequently bioturbated and contain large amounts of mud rip-up clasts.

Distributary mouth-bars are downcut by erosive channels (Fig. 4I) infilled by sets of large-scale (>1 m) trough cross-stratified conglomerates and pebbly sandstones (F21) (Fig. 4J) or occasionally structureless, clast-supported conglomerates (F22) (Fig. 4K) interdigitated with coarse-grained to pebbly sandstones (F9). These incising channels, interpreted as distributary-channels to the underlying delta-front deposits, show coarse-grained basal deposits with abundant mud rip-up clasts (up to 0.8 m diameter) (Fig. 4L) and organic detritus, as well as silicified tree trunks that can be up to 2 m in length (Fig. 4M). There is a characteristic absence of associated finer-grained, lower delta-plain deposits.

Immediately and sharply above the distributary channels dark marine mudstones occur (few tens of metres thick) that have an erosive-based, 10 to 20 cm thick pebbly and shelly basal lag deposit. Because of the basal lag and the extensive occurrence of the mudstones (kilometres) they are interpreted as a marked transgressive interval on top of the shelf-edge delta succession. Further, the mudstone interval contains a series of outstanding whitish sandstone units (10 to 12 m thick) with clear evidence of deposition or reworking by tidal currents because of their strong bi-modal distribution (Fig. 5A) of palaeocurrents. These sand-prone units are built by orderly stacked sets of planar and some trough cross-strata, commonly truncated by reactivation surfaces, and show few mud drapes but some have a configuration of climbing compound dunes. They also contain marine fossils and trace fossils, and are unlikely to be shoreface [no wave indicators like hummocky cross-stratification (HCS) swaley cross-stratification (SWS)] or fluvial units. They resemble the tidal sandbodies commonly occurring on the shelf, in tide-dominated deltas or in estuary mouths (e.g. Stride, 1982; Dalrymple & Rhodes, 1995; Olariu *et al.*, 2012a,b). Subaqueous dunes on modern shelves are sand-prone (e.g. Kenyon *et al.*, 1981; Liu, 1997) whereas those in estuaries have more muddy drapes (Reynaud & Dalrymple, 2011). The tidal dunes are associated with the transgressive mud unit, so a shelf or estuary mouth interpretation is preferred herein, although they could also have been tidally reworked from a new deltaic outbuilding.

Evidence for tidal reworking at the shelf edge

For the uppermost transgressive sandy units the tidal signals and tidal palaeocurrent bi-directionality are clear, but evidence for tidal currents within the river-dominated shelf-edge deltaic units is slimmer. There is a marked rarity of hetherolithic deposits and muddy-stratification (e.g. Longhitano *et al.*, 2012) because of absence of tidal flats, and it is commonly difficult to make the tidal argument in the La Jardinera fluvial to marine transition zone (cf. Dalrymple & Choi, 2007; Shchepetkina *et al.*, 2019). Therefore, instead of being assertive or dogmatic, tidal signals are rather proposed here as a hypothesis and interpreted to occur predominantly in the interdistributary lower delta-plain to upper delta front deposits, based on the following evidence:

Field-based evidence

(i) Foreset palaeocurrent directions (south/south-west) measured within cross-bedded sandstones of the distributary channel-fills show a remarkable number of landward directions, suggesting a net-landward transport of sediment resulting from flood tides; (ii) orderly stacked, planar cross-stratified sandstone sets (up to 20 cm thick) with reactivation surfaces that cut across the foresets (Fig. 5B and C) and display overall bi-modal palaeocurrents (Fig. 5D) with some examples of herringbone cross-stratification in places. Occasionally very fine sand to mud-draped or organic-draped foresets (Fig. 5E). These composite sandstone units are well-sorted and contain marine fossils and trace fossils, and lack significant wave-storm related sedimentary structures (that would suggest upper shoreface) or frequent erosion surfaces (that would suggest fluvial deposits); (iii) presence of compound cross-strata, with smaller dunes climbing obliquely up the stoss sides of larger dunes, something that is common in tidal dune fields and bars, but not in other environments; (iv) increasing–decreasing proportion of muddy rip-up clasts in the stacked dunes, suggesting that there had been more mud deposition than now seen, due to subsequent fluvial erosion.

Theoretical arguments

(i) the overall dominance of tidal influence that is interpreted throughout Lajas stratigraphy elsewhere (e.g. McIlroy *et al.*, 2005; Gugliotta *et al.*, 2015; Rossi & Steel, 2016; Kurcinka *et al.*, 2018); (ii) the absence of storm-wave structures (HCS

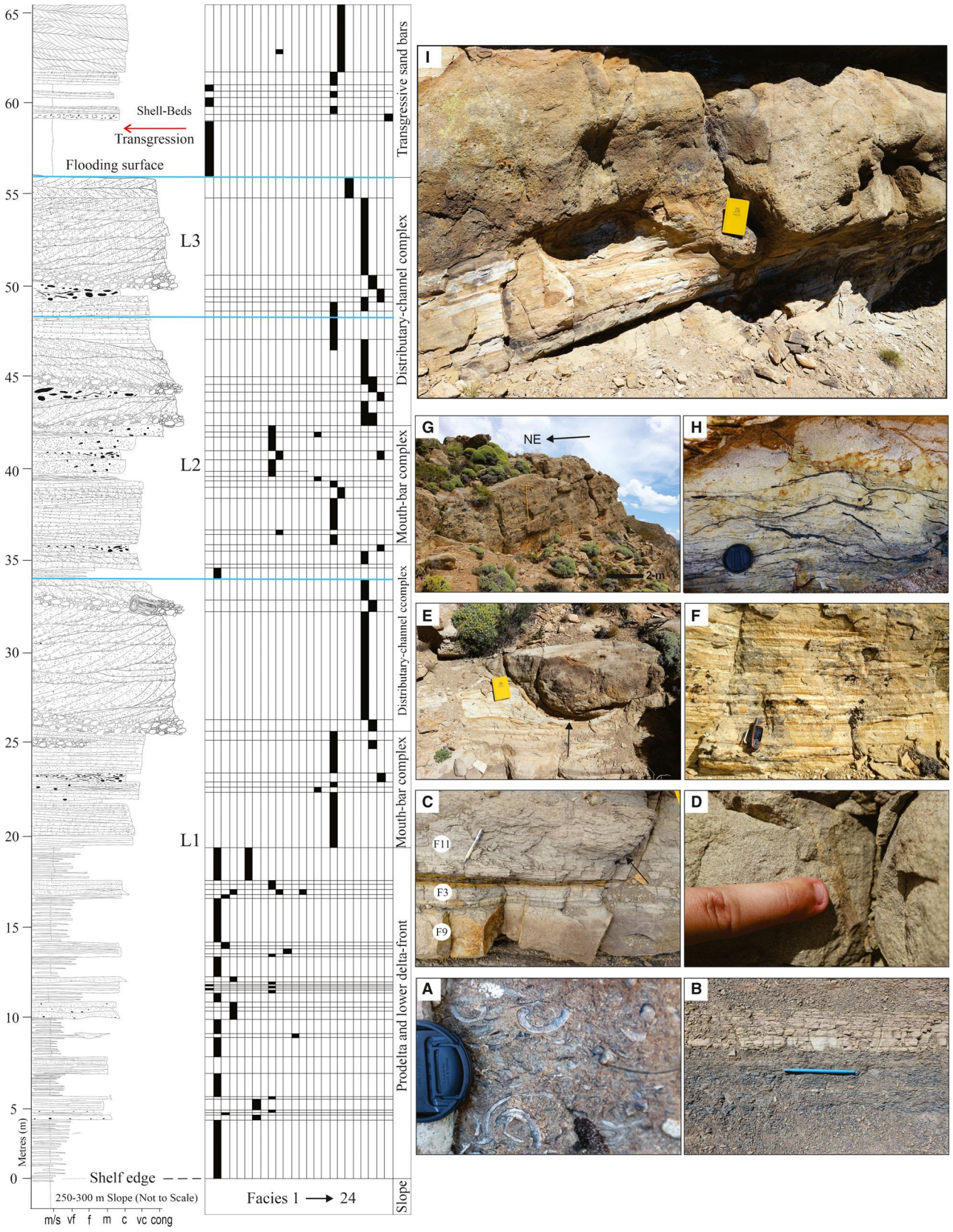

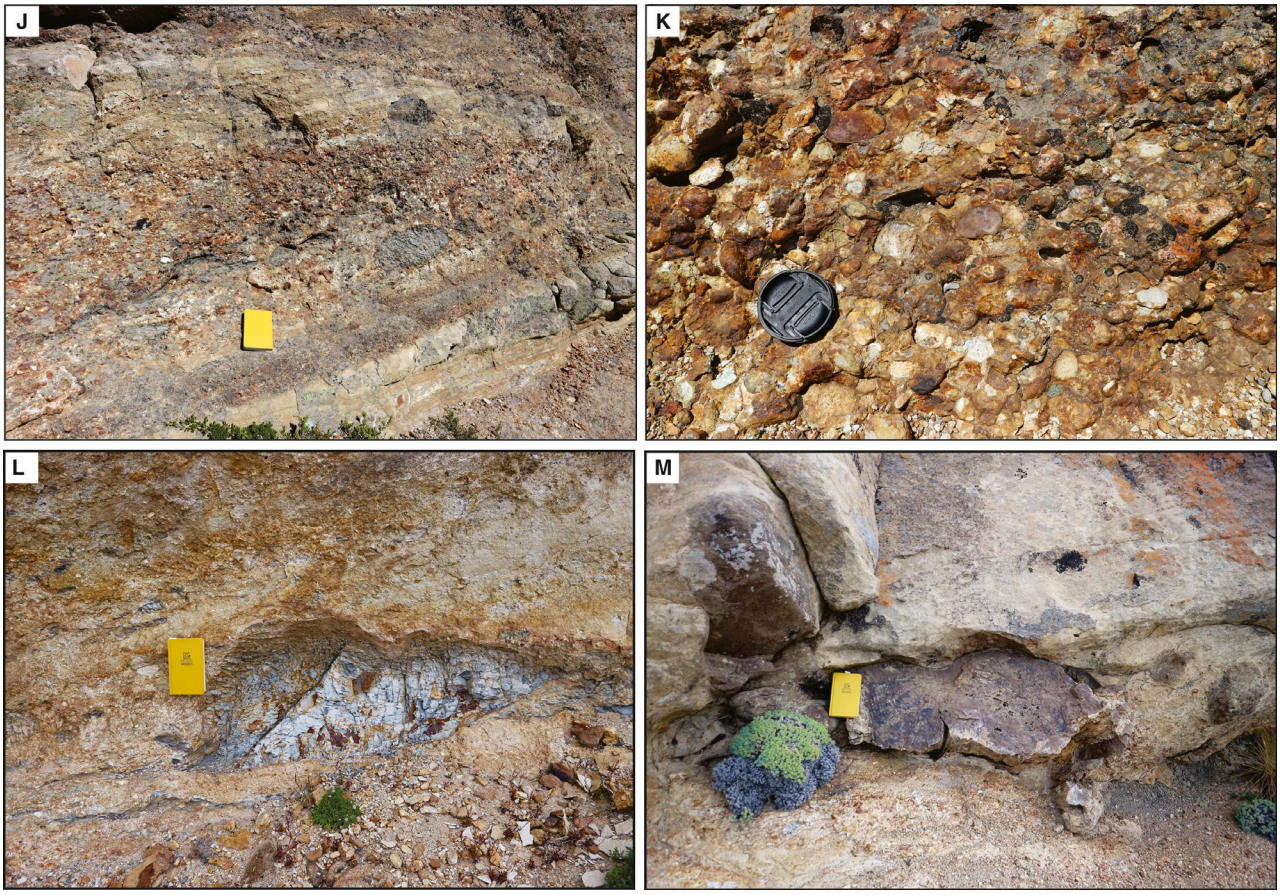

Fig. 4. Detailed sedimentary log that typifies a shelf-edge delta succession together with photographs of the most common facies. (A) Shell-lags at the lower and upper boundaries of the succession. (B) Prodelta mudstones and thin sandstones. (C) Lower delta-front bedset showing from base-to-top: structureless (F9), thin-laminated (F3) and aggrading wave-rippled sandstones (F11). (D) Vertical burrows (*Skolithos* trace fossils) as common occurrences in prodelta and lower delta-front deposits. (E) Collapsed intraformational sandstone block (F12) (upper right) as part of lower delta-front sandstones. (F) Planar-parallel to low angle stratification in medium to coarse-grained sandstones that are characteristic of mouth-bar deposits. (G) Forward-accretion (progradation) pattern in mouth-bar deposits towards the north-east. (H) Organic detritus commonly occurs within inter-sandstone bedsets. (I) Sharp erosive contact between distributary-channel fill (FA4) and mouth-bar deposits (FA3). (J) Large-scale, trough cross-stratified conglomerate to pebbly sandstone as part of a distributary-channel fill. (K) Close-up view of the clast-supported texture of conglomerates within distributary-channel fills. (L) Mud-rip up fragment, 0.8 m in diameter, occurring associated with pebbly sandstones and conglomerates within distributary-channel fill deposits. (M) Silicified tree trunk marking the base of distributary-channel fill deposits. Dimensions of the objects used as scale: (i) lens cap, 5 cm; (ii) yellow field notebook, 19 × 12 cm; (iii) grey and blue pens, 15 cm; and (iv) GPS device, 16 × 7 cm.

or wave ripples) make it clear that tidal signals were not destroyed by waves, as commonly happens on open coasts; (iii) tidal currents are characteristically stronger along the shelf edge zone, because the tidal oceanic wave is compressed when crossing the shallower shelf break area (Fleming & Revelle, 1939); and (iv) the absence of mudstone layers or drapes may be explained by maintenance of sediment suspension due to tidally induced turbulence (Souza *et al.*, 2004).

THE LAJAS SHELF-EDGE DELTAS: ALONG-STRIKE CHARACTERISTICS

The depositional strike-oriented Don Cordero cross-section is composed of three stacked coarsening-upward and shallowing-upward successions representing a 70 m thick shelf-edge deltaic succession, and forms a 5 km long, strike-elongated, wedge shaped fairway belt (Fig. 6). The prograding wedge directly overlies *ca* 250 m

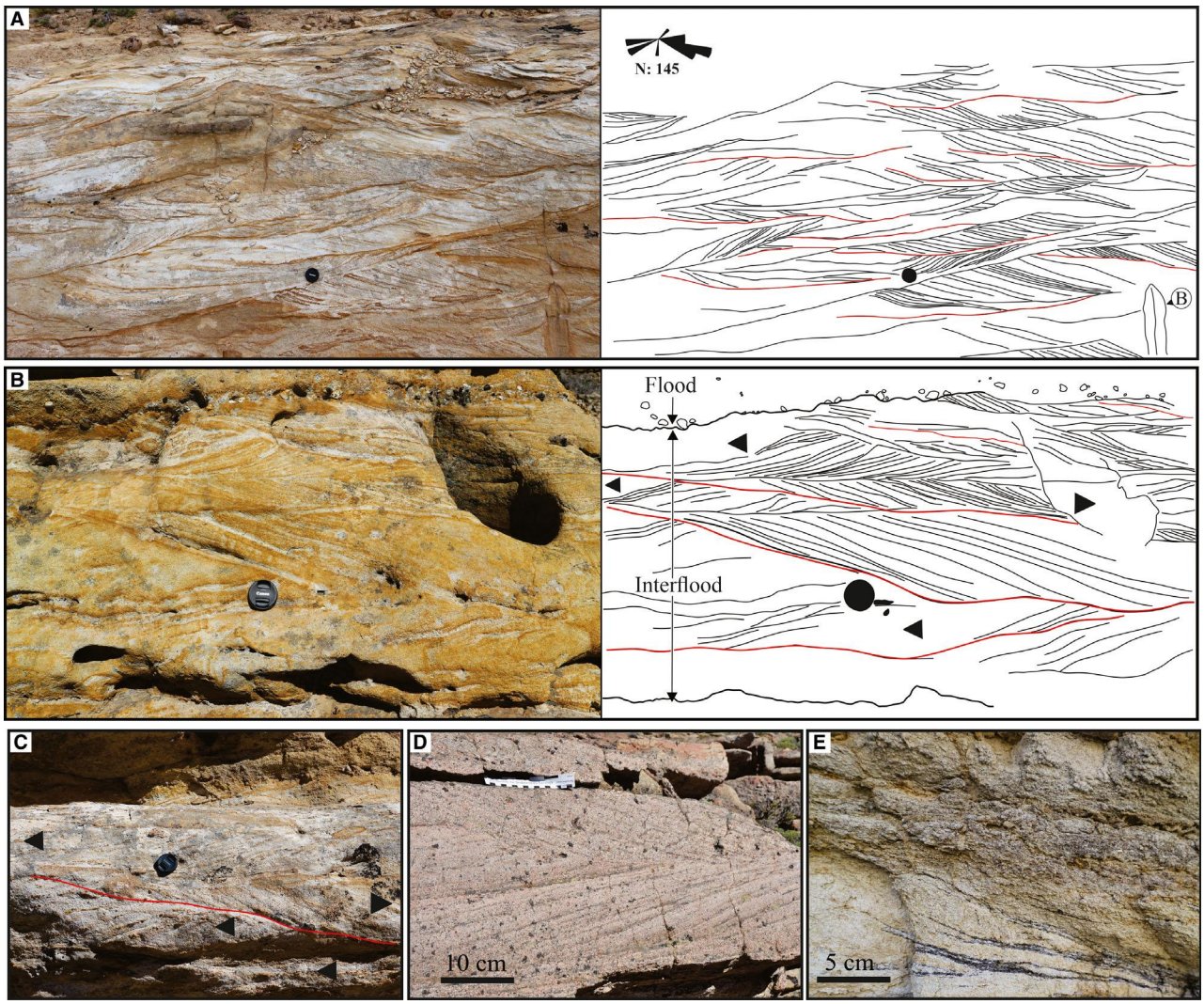

Fig. 5. Interpreted evidence for tidal-reworking. (A) Climbing compound dunes (stoss master surfaces down to the left): 20 to 30 cm dune foresets tend to be unidirectional to the right but adjacent foresets can also be seen to dip in opposite direction. Note the bi-directional character (upper-left rose diagram) of these compound dunes. (B) Interpreted flood–interflood association in lower-delta plain to upper delta-front deposits. Interflood deposits display a complex organization of opposite dipping foresets that can be truncated by reactivation surfaces, while flood associated deposits are massive. This association suggests tidal reworking between river floods. (C) Stacked sets of planar cross-stratification showing bi-directional foresets that are commonly truncated by reactivation surfaces. (D) Another example of opposite dipping foresets. (E) Very-fine sand to mud-draped and/or organic-draped foresets. Legend: Red lines represent reactivation surfaces; B = bioturbation; black arrows: palaeoflow direction. Dimension of lens cap used for scale is 5 cm.

thick, deepwater mudstones and is overlain by tens of metres of outer-shelf offshore mudstones. Lateral pinch-out of the main distributary-channel fairways (yellow arrows, Fig. 6) suggests that the distributary channel belts have a spacing of a 1 to 2 km and are separated by lower-energy inter-distributary tracts along the shelf-edge.

The individual distributary fairways in each of the three coarsening and shallowing-upward successions is interpreted to represent a prograding deltaic lobe, and the group of three upward-coarsening successions forms a clinothem set, here namely from base-to-top as L1, L2 and L3. By application of Walther's law, older to younger coarsening and shallowing-upward successions prograded over one another and therefore give insight on along-strike and proximal–distal facies and architecture

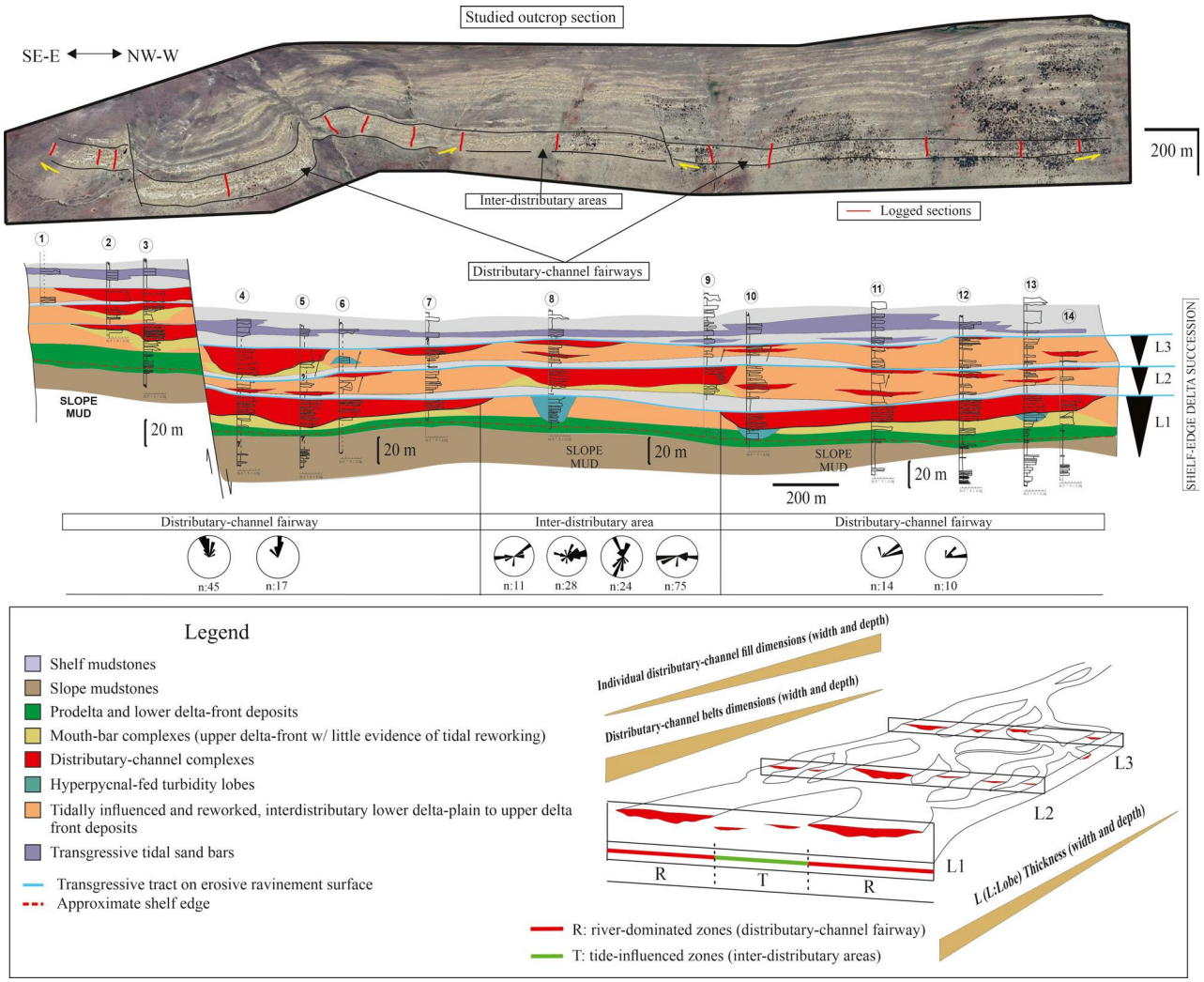

Fig. 6. A *ca* 5 km correlated transect, along depositional-strike (Don Cordero), straddling the shelf–slope break in southern part of the study area. Black lines comprise the *ca* 70 m thick studied stratigraphic interval. The facies suggest coarse-grained, river–tide interaction shorelines at or near the shelf edge. Distinction between the main distributary-channel fairways and inter-distributary areas is shown for upward-coarsening succession/delta lobe 1 (L1). Note that while distributary-channel fairways exhibit strong unidirectional palaeocurrent indicators, inter-distributary areas exhibit bi-modal palaeocurrent interpreted to result from tidal reworking. The proximal–distal association (L3 to L1) suggests widening of distributary channel-belts basinward (towards the shelf edge): L1 upward-coarsening succession/delta lobe 1; L2 upward-coarsening succession/delta lobe 2; and upward-coarsening succession/delta lobe 3; yellow arrows = lateral pinch-out.

variability within a shelf-edge deltaic succession (see panel correlation, Fig. 6).

Architecture variability of depositional elements along depositional-strike-oriented shelf-edge deltaic succession

Distributary channel-belt complexes

The stacking and merging of individual distributary-channel complex fills (FA4) form composite coarse-grained, distributary channel belts (red coloured in Fig. 6). These channel-belts change their architecture (width and depth scales) from L1 up to L3:

1 *L3 and L2*: Distributary channel belts are 150 to 600 m wide and 5 to 15 m deep, and distributed in a scattered way.

2 *L1*: Crudely, upward-fining distributary channel fills cluster in channel-belts that can reach up to 25 m thick and 0.8 to 1.3 km wide. Importantly, between channel belts there are 1

to 2 km wide, finer-grained inter-distributary deposits. Within the inter-distributary channel belts there are also metre to decametre-scale, channel fills or lags isolated in fine to medium-grained sandstones and siltstones. The along-strike sedimentary panel shows two main coarse-grained channelized complexes, with intervening finer grained segments, i.e. the main delta fairway had several distributary channels as well as inter-distributary areas.

3 *In L1*, shelf-edge channel belts are formed by a complex interfingering between individual distributary channel fills and mouth-bar deposits (Fig. 7A).

Although channel belts in L1 are wider and deeper than those within L3 and L2, individual distributary channel fills (FA4) tend to be wider and deeper (up to 7 m thick and tens to hundred metres wide) in L3 and L2, compared to their L1 counterparts (up to 5 m thick and tens of metres wide) (Fig. 7A). It is important to note that channels incise 10 to 15 m into their own delta front, but do not cut down as far as the previously deposited upward-coarsening succession.

Distributary-mouth bar complexes

Sandstone bodies up to 10 m thick and hundreds of metres in width, non-channelized but sharp to slightly erosive at times, consisting of upward-coarsening stacked bedsets that internally display gently basinward-dipping (to the NNE) lamination with some mud drapes and carbonaceous drapes, as previously described. These mouth-bar deposits amalgamate laterally along strike to develop hundreds of metres to kilometres extensive, delta-front sandstone belts characterizing distributary-mouth bar complexes. Sandstone belt thicknesses may drastically vary, along both depositional strike and dip, commonly reaching less than 3 m thick due to partial cannibalization by the downcutting distributary-channel complex fill deposits (Fig. 4I).

Interdistributary lower delta-plain to upper delta front sandstone belts

These deposits form up to 15 m thick and hundreds of metres wide, composite sandstone units that are along-strike elongated and deposited between the main distributary-channel belts. Consists of fine to coarse-grained sandstone packages that mostly show: (i) orderly stacked, cross-stratified sets (up to 20 cm thick) with bi-modal palaeocurrents, with the presence of fine-sand to mud-draped or organic-draped foreset bundles (FA6) (Fig. 5B and E); and (ii) 0.1 to 0.3 m thick trough cross-bedding, sometimes containing up to 2 cm scattered pebbles (F20). Sandstone packages show lobate to sheet-like geometries. Secondary facies include flat-laminated and structureless sandstones, as well as thin-bedded (<10 cm thick) mudstones and sandstones, but these represent less than 20% of the association. The thin-bedded intervals are often current ripple laminated, occasionally climbing. Co-sets of planar cross-strata, the majority of the occurrences, bi-modal foreset directions and reactivation surfaces that cut across the foresets. Composite sandstone units are cut by clast-supported orthoconglomeratic packages that are characteristically trough cross-stratified and channelized (FA4). Such channelized conglomerate units (<4 m thick) are, however, much smaller than the large-scale channel belts (Fig. 5B, close-up view of tidally reworked facies within distributary channels).

Hyperpycnal-fed shelf lobes

Especially associated with L1, probably the most distal, outer-shelf unit, non-channelized sandstone bodies occur with relatively flat lower-bounding surfaces that display aggradation along with marked lateral accretion (Fig. 8). They constitute homogeneous, sharp-based, and well-sorted (containing no conglomerate clasts) fine-grained to predominantly (>70%) medium and lower coarse-grained, flat-laminated and stacked sandstones (F15) up to 15 m thick (FA5), with individual beds up to 1 m thick. Secondary facies include centimetre-scale, shear-induced bedding deformation and occasional ‘scour and fill’ cross-beds (F10). Two distinctive features of importance are: (i) the simultaneous occurrence of normal and inverse lamina-set grading (upper-right, Fig. 8); and (ii) individual laminae, beds and bedsets are laterally extensive at outcrop scale, from metres or decametres laminae, beds and bedsets to hundred metres composite bedsets. These sandstone bodies have been interpreted by Steel *et al.* (2018) as small hyperpycnal shelf fans built in front of small rivers that did not reach the shelf break. Note that lobes seem to stack basinward, likely indicating north-east progradation (Fig. 8).

Sheet-like, thin sandstones or lithosomes

Up to 1 m thick and tens of metres in lateral extension, sheet-like and stacked sandstone bedsets embedded and restricted within the

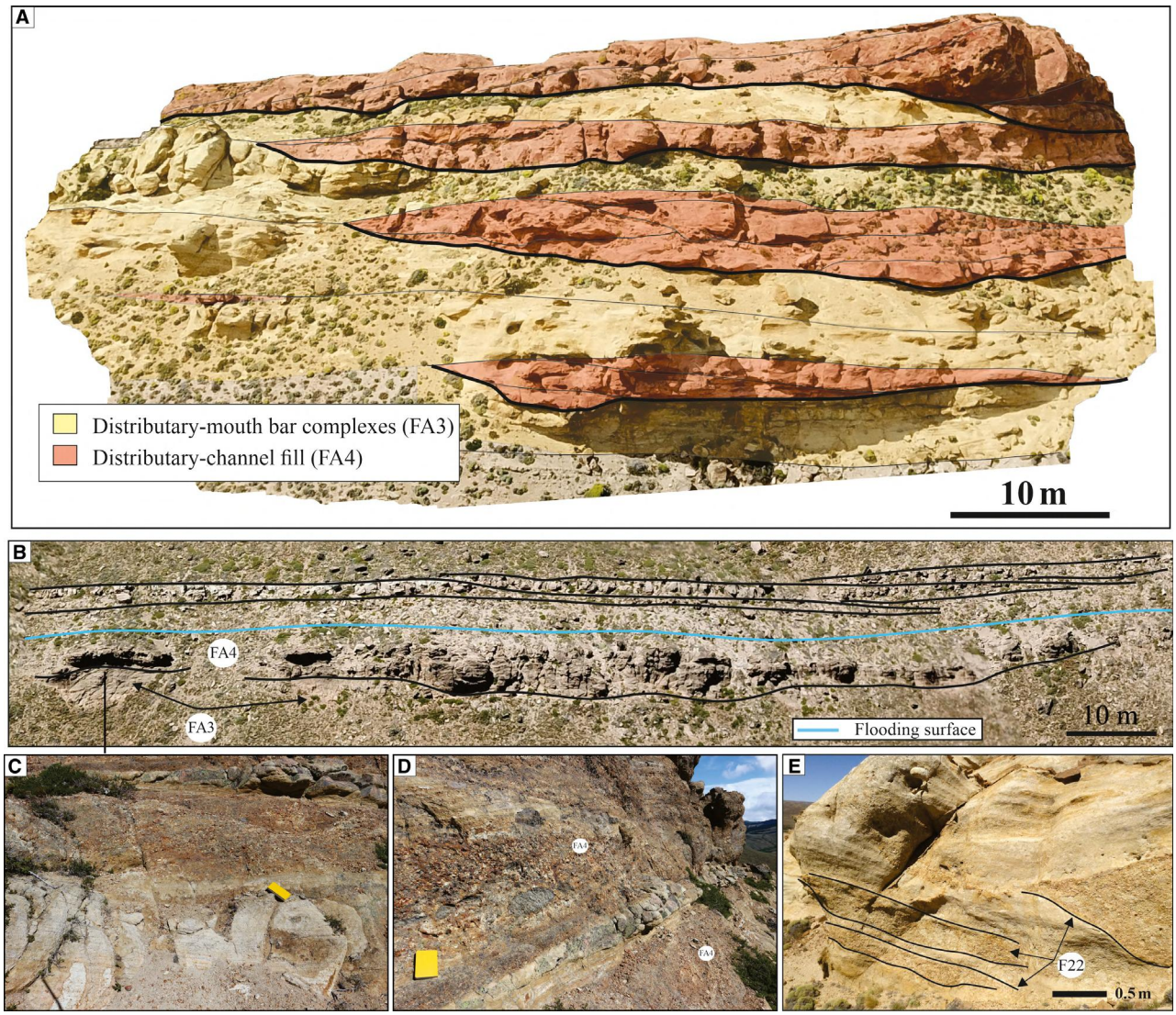

Fig. 7. (A) Coalescence of small-scale channel fills and mouth-bar deposits within a larger-scale (not included in the photograph) channel-belt. Note that individual channel fills are deeper and wider upward. (B) Outcrop expression of the erosional contact between distributary channel fills and mouth-bar sandstone belts typifying a distributary channel-belt and mouth-bar sandstone belt association. (C) Contact between flat-laminated sandstones of distributary mouth-bar deposits and trough cross-stratified conglomerates of distributary channel fills. (D) Zoom out on (C), where there is large-scale (1.5 m) trough cross-stratification in conglomeratic units. (E) Chute channels (i.e. terminal distributary-channels) cutting on top of mouth-bar sandstones. Dimension of the yellow field notebook used as scale is 19 × 12 cm.

lowermost shelf-edge prodeltaic to uppermost slope mudstone units. These sandstone units become thinner (<40 cm thick) or pinch-out laterally and become more thin-bedded with siltstones towards inter-distributary areas.

Lateral process mix in the shelf edge deltas

The lateral facies variability along the shelf edge indicates that the main distributary fairways were consistently river-dominated, while inter-distributary deposits exhibit evidence of tidal reworking. Storm-wave signals are rare but occasionally occur across both distributary and inter-distributary areas. This represents much less wave influence than is documented for storm-wave influenced shelf-edge deltas elsewhere (e.g. Covault *et al.*, 2009; Dixon *et al.*, 2012b; Peng *et al.*, 2017), indicating that waves and storms caused only minor reworking of sediment

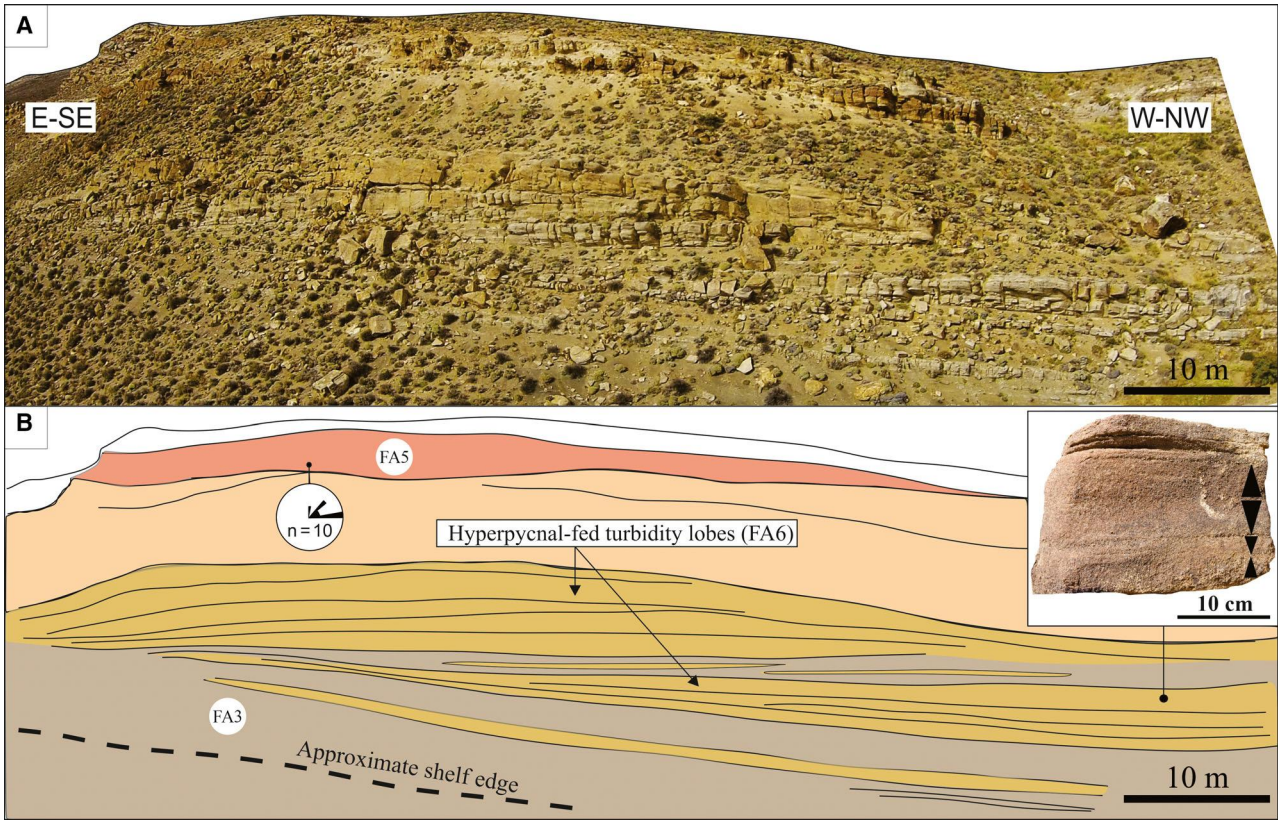

Fig. 8. Outcrop expression and architectural framework of stacked hyperpycnal-fed shelf lobes. (A) Composite drone photographic panel along depositional-strike cross-section (Don Cordero Estancia). Hyperpycnites (lowermost sandstone units) are overlain by tidally-reworked delta front mouth-bar and terminal distributary-channel fills (FA4) forming an upward-coarsening regressive sequence. (B) Interpretation of sandy hyperpycnal shelf lobes suggests the location where gravelly dispersal did not reach the shelf edge or where the sandy shelf lobes were simply forerunners of the over-riding gravelly deltas. Lobes show apparent basinward stacking (towards the north-east), and also exhibit lateral aggradation/accretion. Note that sandstones display lamina-set grading at bed-scale (upper-right in the figure).

at the river mouths. Although waves represent a weak secondary process here, the relative absence of mudstone layers suggests that wave-reworking was enough to keep the fine sediments in long-term suspension. These deltas are therefore interpreted here as river-dominated and tide-influenced (e.g. Ainsworth *et al.*, 2015; Rossi & Steel, 2016) because of: (i) the dominance of erosively based, very coarse-grained, trough cross-stratified distributary-channel deposits, along the main distributary fairways, over-reaching the shelf edge; (ii) the presence of along-strike (inter-distributary), orderly stacked tidal dunes (mainly stacked planar cross-strata with bi-directional palaeocurrents) in thin units of fine-grained sandstone and occasional sandy conglomerate, caused by tidal-current reworking in the inter-distributary areas; and (iii) the prominent presence of laterally-extensive, low-angle stratified, upward-coarsening river-mouth bars, with only occasional tidal signals, below the main distributary channel deposits.

The differing architectural characteristics between L1 and L2/L3, assuming an overall progradation of the 70 m thick shelf-edge delta complex, suggest that the widest and deepest-cutting channel belts occupied the outer shelf zone closest to the shelf edge, although individual distributary channels farther back from the shelf edge could be as deep or deeper. Along reaches of the outermost shelf that were less well fed, without channel belts or inter-distributary bays, smaller less competent rivers dumped gravel at their mouths but dispersed low-density hyperpycnal turbidites to form sand lobes on the outermost shelf.

Such along-strike variability of river-dominated and tide-influenced zones in shelf-edge deltas has

also been interpreted in the Permo–Triassic Karoo Basin in South Africa (Laugier & Plink-Björklund, 2016). In other cases of tide-influenced shelf-edge areas, with only dip-oriented sections, strong tidal signals were widespread even along the delta distributary channels (e.g. Cummings *et al.*, 2006; Schwartz & Graham, 2015). Although examples of tide-influenced shelf-edge deltas are scarce for comparison purposes, all share an important characteristic, namely the rarity or lack of storm-wave deposits. Tide-influenced shelf-edge deltas, therefore, likely indicate areas in which waves were attenuated and tidal currents amplified, such as, for example, within structural embayments, or canyons (e.g. Archer & Hubbard, 2003; Cummings *et al.*, 2006; Plink-Björklund, 2012). The topographic anisotropy created due to differential subsidence between blocks and depocentres in the Early–Middle Jurassic sub-basins in southern Neuquén Basin (Vergani *et al.*, 1995; Kim *et al.*, 2014) likely created protected embayments with enhanced tidal currents, such as in La Jardinera area.

These observations indicate that the main Lajas distributary channel belts were kilometre-wide coarse-grained composite units placed near or at shelf-edge sites, although replaced by hyperpycnal shelf-fan lobes in places where the distributaries terminated before reaching the shelf break. The distributary sandbelts are likely to be important zones of sand bypass to deepwater areas of Lajas–Molles margins. Interdistributary areas with composite sandy units reworked and remobilized by tidal currents would have contributed to this downslope sand supply only when avulsed distributary channels occasionally swept into the inter-distributary areas.

THE DOWN-DIP EXPRESSION OF SHELF-EDGE DELTAS AND TRANSITION TO DEEPWATER SLOPE CHANNELS

Based on sedimentary log correlation along depositional-dip section in Bey Malec Estancia (Fig. 9), at a lower stratigraphic level (Toarcian; Daniel Minisini, pers. comm.) than the depositional-strike section discussed above, a six-clinothem stratigraphy has been mapped (identified as '1' to '6' in Fig. 9C and D). Imaged clinoform slope geometries are typified by repeated low-angle (4 to 6°, see Olariu *et al.*, 2019), downslope penetrations of coarse-grained Lajas deltaic deposits (channelized conglomeratic and coarse sandy units) into the coeval, muddy Los Molles Formation.

Because there is always some uncertainty in reconstructing clinoform stratigraphy, it is correct to ask whether, instead of 'timelines', channels could simply be randomly arranged on a muddy slope succession. The key evidence that this is not the case and that channels are broadly lining up along timelines, is that viewing by eye, by drone photography and by high-resolution satellite image strongly indicates that they correlate down through an otherwise relatively muddy slope succession (Fig. 3). In addition, this is confirmed by walk-out examination, where clinoforms can be seen to begin as delta-distributary channel facies at the shelf edge (see next sections), but persist as continuous or closely spaced (submarine-slope channel fills) gravity-flow deposits down throughout the slope mudstones. Moreover, the main evidence that the correlation timelines are not flat but are inclined timelines within a muddy slope is that the picked timelines diverge downslope from their point of intersection with the flat-lying topset deposits. These timelines begin proximally at the shelf edge area, but after several kilometres they diverge from the overlying flat-lying topset datum by >150 m vertically (Fig. 3B).

Furthermore, in the Bey Malec area, the updip correlation of these coarse-grained horizons shows that they do not merge landward into topset strata, but become toplap truncated by a transgressive surface that hosts sandy lag deposits and overlying thin sandstones embedded into an approximately tens of metres thick, muddy marine transgressive interval. The latter mudstones are associated with a major (several kilometres) transgressive landward shift of the shoreline, which then turned around to regression (prodelta deposits, followed by delta front and downcutting delta distributary-channels) as the rebuilt topset at higher stratigraphic level. This outcrop area thus demonstrates a large-scale example of topset-eroded oblique clinothems (cf. Mitchum *et al.*, 1977) (Fig. 10). Topset erosion cannibalized much of the inner deltaic successions, with only the most basinward reaches of deltaic deposits being preserved in clinothems 3 to 6, where the shelf–slope transition strata are captured by the logged sections.

Down-dip and vertical facies architecture along the shelf–slope break transition (clinothems 3 to 6)

Shelf-edge distributary channels show a downslope change from stratified conglomerates with

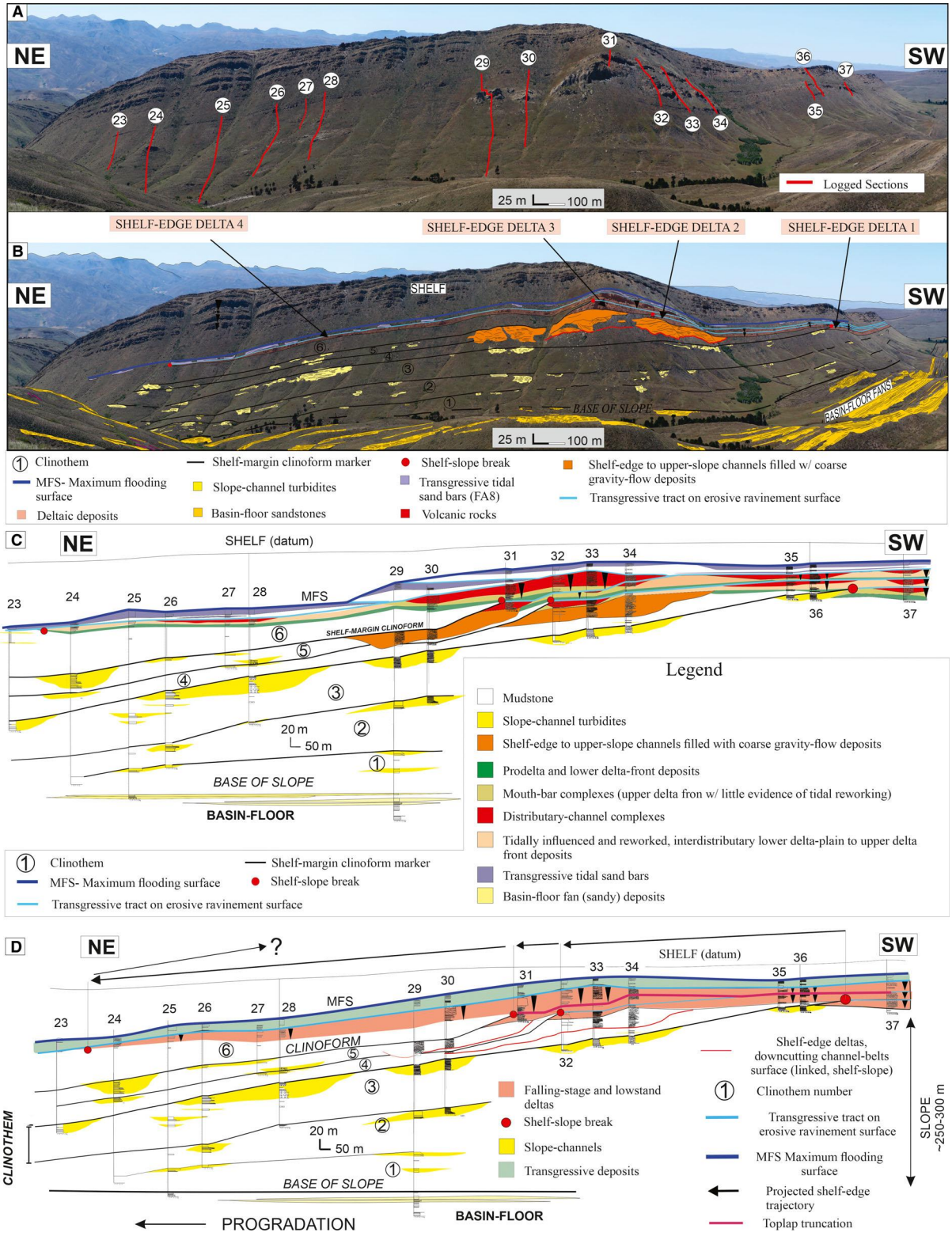

Fig. 9. Sedimentary log correlation along depositional-dip cross-section (Bey Malec Estancia). (A) Position of the logged sections. (B) Cross-sectional sketch of the area. (C) Stratigraphic correlation between the measured sections showing the delimitation of the six mapped shelf-margin clinoforms and clinothems, and facies association distribution. (D) Sequence stratigraphic framework with possible indication of falling-stage shelf-edge trajectory (1.4 times vertical exaggeration is applied in all figures for better visualization).

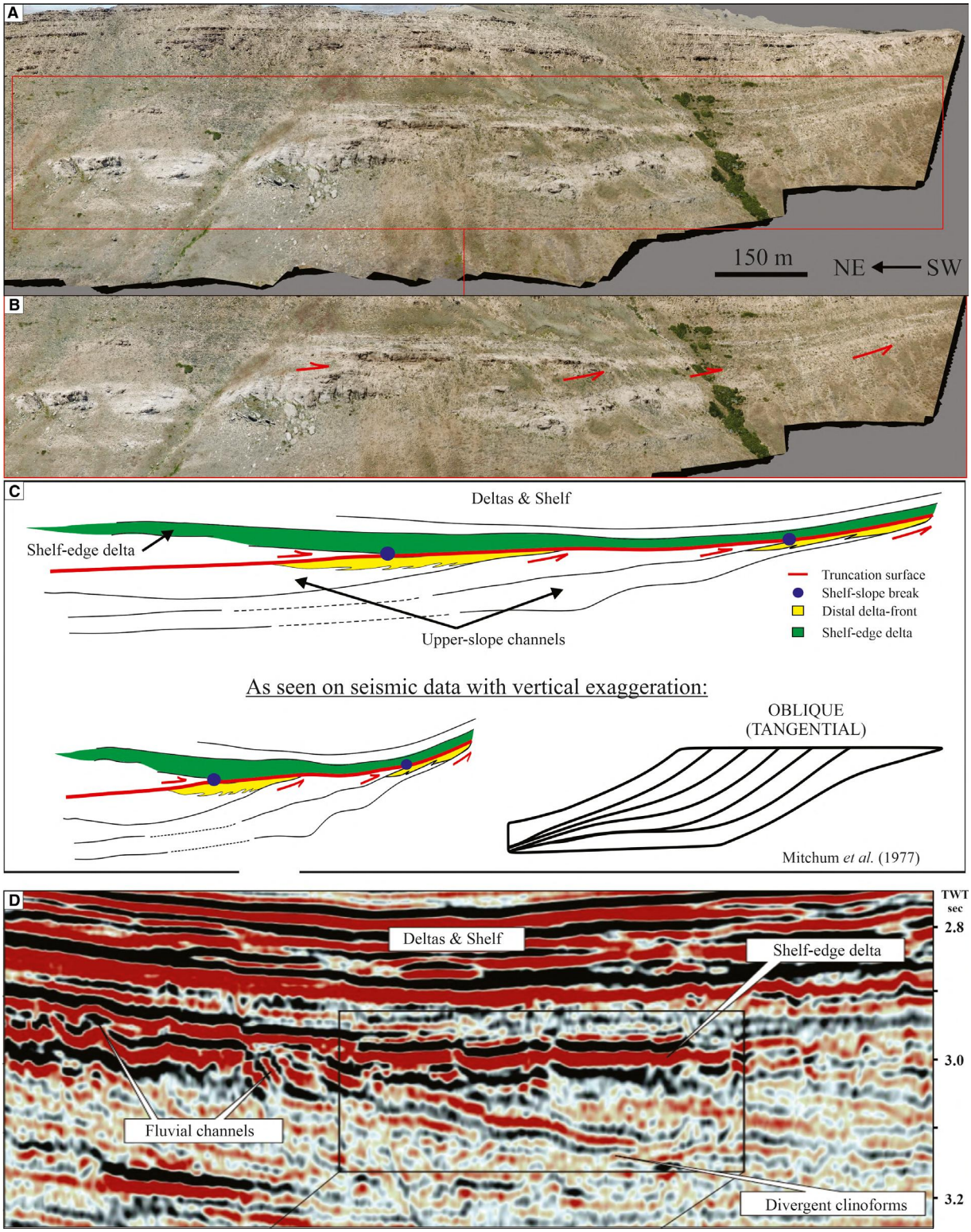

Fig. 10. (A) Outcrop view of an oblique-type, shelf-margin clinoform set along depositional-dip Bey Malec cross-section. (B) Toplap truncation indicated (red arrows), which can be easily seen from the divergent angle of strata. (C) Interpretation showing the oblique-type, clinofom set (*sensu* Mitchum *et al.*, 1977). (D) Identical situation, but oblique-type clinoform set is now seen from seismic data. The black square highlights such geometry (from Johannessen & Steel, 2005).

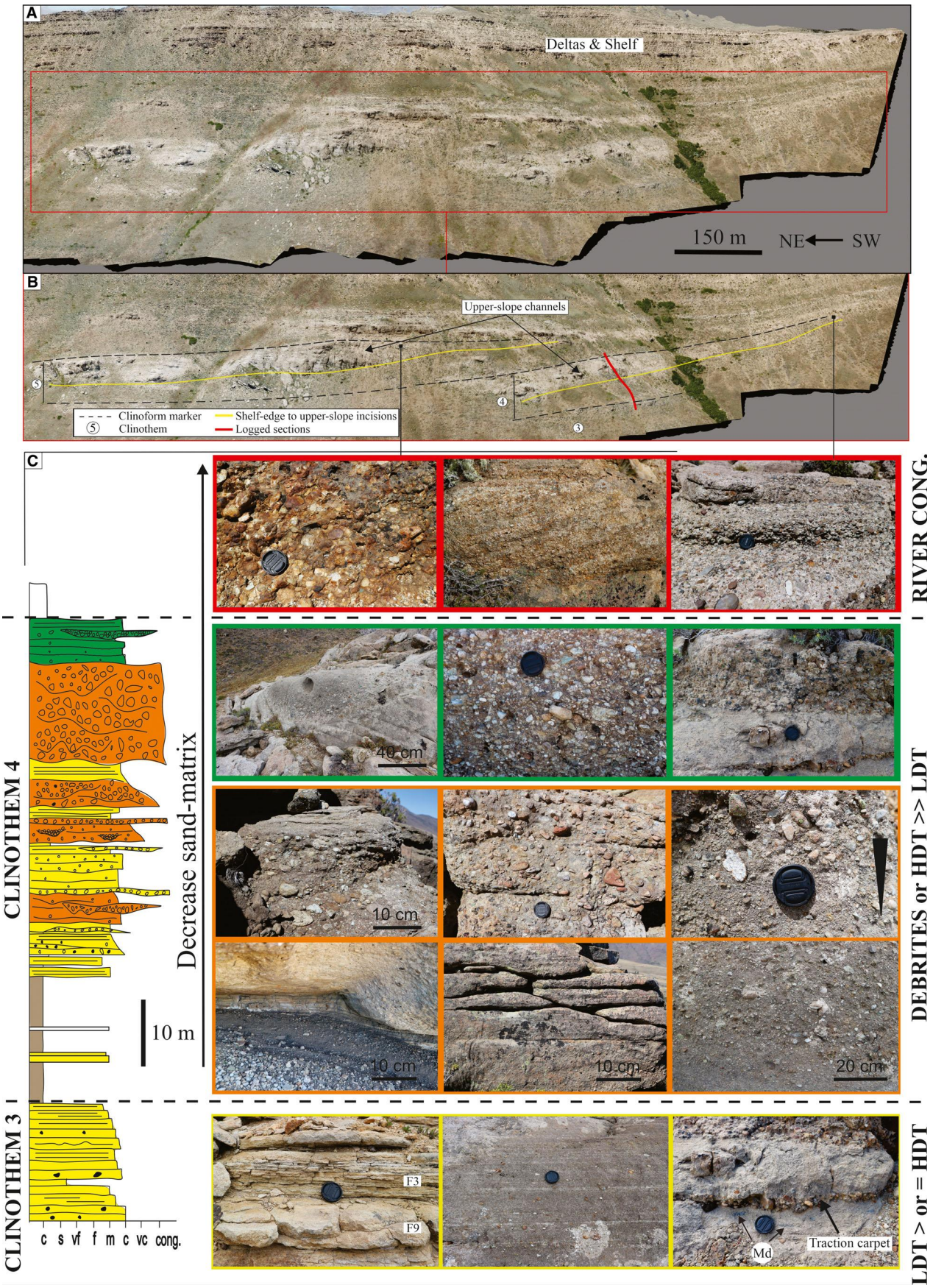

Fig. 11. Facies and architecture along the shelf–slope break deposits in clinothems 4 and 5. (A) Outcrop view of upper-slope channels (tongues within the Los Molles mudstones). (B) Interpretation of large-scale architecture of the shelf–slope break, highlighting the incisions (yellow lines). (C) Sedimentary log capturing clinothems 3 and 4. Clinothem 3 deposits represent intermediate slope-channel fills with marked occurrence of high-density and low-density turbidites (HDT and LDT). In the case of clinothem 4, however, the logged section captures the uppermost slope-channel deposits. Note the upward decrease in sand-matrix. This interval is predominantly dominated by debrites and high-density turbidites (HDT). The textural variation of conglomeratic units seen along the section is displayed using colours. (Yellow: intermediate slope-channel turbidites; Orange: uppermost slope-channel debrites and high-density turbidites; Green: distal deltaic wedges on uppermost slope to shelf edge sites; Red: river stream flow deposits. Dimension of lens cap used for scale is 5 cm.

relatively well-sorted, clast-supported gravels with minimal sand matrix (as is common in river channels, e.g. see Nemec & Steel, 1984) to poorly sorted, mainly sand-matrix-supported unstratified debrites and high-density turbidites of slope settings. However, there are marked changes in facies stacking patterns and upslope–downslope distribution, as well as shelf–slope break architecture in each clinothem. The next sections provide descriptions and interpretations of the shelf–slope break deposits in each clinothem.

Clinothem 3

Clinothem 3 is overall upward fining and can be walked out from the shelf-break to a kilometre below the shelf-break, and is channelized. Near the shelf break it is characterized by 1 to 5 m thick bedsets vertically stacked into composite bedsets that can reach up to 20 m thick. Bedsets consist primarily of structureless to normal graded and laminated sandstones (F3), structureless to graded sandstones with floating pebbles (F4), sandstones with basal clast-supported conglomerates (F5) (pictures on yellow colour chart, Fig. 11). Bedsets are separated from one another by 5 to 20 cm thick intervals of thin-bedded (<10 cm thick), laminated mudstones and sandstones (F2), and sometimes by an erosive surface that marks an abrupt change in grain size. Laminated sandstone beds are medium to lower coarse-grained and irregularly flat-laminated with tabular to irregular sharp bases. Structureless sandstones, amalgamated with erosive bedset contacts, are 0.2 to 0.8 m thick, from upper medium-grained to conglomeratic. A distinctive aspect of these sandstone units is the occurrence of considerable amounts of gravels (up to 10%), which does not happen in the laminated sandstone units. Floating pebbles [maximum particle size (MPS) = 0.5 to 3.0 cm], and clast-supported conglomerates form discontinuous sand-matrix to clast-accumulations (MPS = 0.3 to 4.0 cm). Mud rip-up clasts are common at the base of bedsets and some beds. Organic fragments are rare.

Interpretation. The sharp bases of beds and bedsets associated with the characteristic aggradational stacking in this clinothem indicate repeated cutting and filling of channels. The turbidite deposits are interpreted as the infills of channels that are sited, according to the outcrop, on the uppermost parts of the deepwater slope (see also Gan *et al.*, 2019).

Clinothems 4 and 5

The shelf–slope break deposits in both clinothems 4 and 5, form sigmoidal-like sand to conglomeratic bodies that extend tens to hundreds of metres downslope thickening and thinning (up to 40 m maximum thickness), and have slightly irregular erosive bases with the underlying marine mudstones (Fig. 11). The up-dip terminations of both sandstone bodies show an increased occurrence of up to 1 m thick and 4 m wide channelized, and sometimes flat-stratified, clast-supported conglomerate units (red squares, Fig. 11C). There is a consistent upward decrease in sand matrix within sandstone to conglomeratic bodies, where sand-matrix-supported conglomerates and pebbly sandstones change upward, even though contacts are characteristically sharp, into clast-supported conglomerates (log, Fig. 11C). The base-to-top infill type of an individual sand body within a single clinothem consists of:

1 *Basal unit*: conglomeratic sandstones and sand-matrix-supported conglomerates with some portions being more pebble rich than others, Sandstones with floating pebbles predominate, though there are also some conglomerate units which are characteristically sand-matrix-supported (see yellow and orange colour, Fig. 11);

2 *Intermediate unit*: sand-matrix-supported conglomerates and conglomeratic sandstones that interdigitate with lenticular-like, clast-supported conglomerate units that are poorly flat-stratified at times. Sand-matrix-supported

conglomerate units may show inverse graded beds (orange colour, Fig. 11).

3 *Uppermost unit*: dominance of clast-supported conglomerates which are predominantly flat-stratified or structureless, to occasionally cross-stratified (green colour, Fig. 11).

Interpretation. The erosional downcutting into the underlying mudstones and the downslope thickening and thinning of the sand bodies, together with their mapped and interpreted physiographic position within clinothems, suggest that these sand bodies represent uppermost slope channel fills (Hubbard *et al.*, 2014). The slope-channel, thick pebbly sandstone and conglomerate beds broadly correspond with what was called 'fluxoturbidites' (discontinuous fluxing with 'grain flow' in base of flow) in the Polish Carpathians by Dzulynski *et al.* (1957), Dzulynski *et al.* (1959) and Carter (1975). European fluxoturbidites were later renamed high-density turbidites in a key paper by Lowe (1982), and lately also named sandy debrites by Shanmugam (1996). Upslope–downslope partitioning of sandy and gravelly beds, typified by a downslope increase in the sand/conglomerate ratios, consistently represents the sand–gravel bipartition expected within these flows as demonstrated from flume experiments by Postma *et al.* (1988). The metre-scale and channelized, clast-supported and stratified conglomerate units at the up-dip terminations of both sand bodies are interpreted as deltaic terminal distributary channel deposits that reached the uppermost slope settings. The vertical textural changes are likely due to more catastrophic, matrix-rich sandy debris flows in the channels being possibly reworked by inter-flood stream flows during longer periods. The interfingering/alternation of sand-matrix and clast-supported conglomerates represents evidence of pulsed flooding and a 'gradual' transition, and suggests no collapse in such areas (contrasting collapsed examples can be seen from, e.g. Moscardelli *et al.*, 2006). Therefore, these channel-like features were likely created by erosive submarine gravity flows rather than by mass wasting events (for example, collapses or slumps) (Dakin *et al.*, 2013).

Clinothem 6

In contrast to clinothems 3 to 5, clinothem 6 does not contain sharp-based, upper-slope sandstone units in the outcrop area. The up-dip, shelf-edge deltaic units display reliable evidence for tidal reworking, with same characteristics as described for FA6 and inter-distributary sand belts.

Interpretation. The cross-sectional profile probably transects an inter-distributary area at clinothem 6, as indicated by tidal signals presented in the most basinward deltaic deposits, with only slope lithosomes recorded downslope from the inter-distributary areas.

DISCUSSION

Delta distributary channels at the shelf edge area in continuity with slope channels

The basinward change in the architecture of channels, from wide and deeply channelled distributary belts at the shelf edge to narrower and slightly shallower ones further back on the shelf as interpreted from the strike-oriented shelf edge diagram (Figs 6 and 7A) suggests the coalescence of river drainages at the shelf edge. Convergence of delta distributary-channels near or at the shelf edge has been documented elsewhere from seismic studies (e.g. Perov & Bhattacharya, 2011; Sylvester *et al.*, 2012; Paumard *et al.*, 2018), as well as from analogue tank experiments (Kim *et al.*, 2013), but lacks documentation from previous outcrop studies. Kim *et al.* (2013) have attributed such basinward change in distributary channel patterns to increased gradient and accommodation at the shelf edge. Other controls, for example involving discharge losses 'downstream' (Tooth & McCarthy, 2004) and the non-linear interaction between river discharge and opposing flood tides (e.g. Sassi *et al.*, 2012; Hoitink *et al.*, 2017) likely led to a change in the coastal morphology from river-dominated to tide-dominated parts. The outcrop expression of discharge losses 'downstream' leads to a reduced scale of individual distributary-channels at the shelf edge, even though they coalesce to form wider composite channels–belts than their shelfal counterparts. Seaward widening of composite channels occurs in fluvial–tidal paralic systems due to increased impact of tidal currents (Leuven *et al.*, 2018). The aforementioned aspects are interpreted here to not only have controlled sedimentary architecture of the shelf-edge deltaic units but, most importantly, probably modulated sediment dispersal through preferential routes (i.e. along the main-distributary fairways).

Following the channels further down onto the slope at La Jardinera, it is observed that: (i) upper-slope channels with up-dip terminations at the shelf edge merge with the delta terminal distributary channels, with the exception of clinothem 6;

and (ii) the uppermost slope area lacks significant soft-sediment deformation, collapsed or slumped strata. This suggests that shelf margins in La Jardinera were not primarily collapse/slump-dominated delivery systems, quite unlike those described by Dixon *et al.* (2012a), Laugier & Plink-Björklund (2016) or by Peng *et al.* (2017). The La Jardinera systems rather represent channelized sediment delivery at the shelf edge, initiated at the subaqueous river mouths (because of marine fossils and ichnology, together with no evidence for subaerial exposure in the incised lowermost delta front) that over-reached the shelf break, and directly fed into upper slope channels, such as described by Mellere *et al.* (2002), Plink-Björklund & Steel (2004), Moss-Russell (2009) and Silalahi (2009). Quite simply, the textural and bedding changes of conglomerates from dominantly clast-supported and stratified downslope to dominantly matrix-supported and unstratified, are the most important indicator of transformed flow conditions from shelf to deepwater slope. However, as noted above in the description of the uppermost-slope channel fills, the subaqueous river-mouth areas were subject to long fair-weather periods when reworked and sorted framework gravels could cap the earlier flood generated sandy debris flows, generating an interfingering of mature and immature gravels. This apparent 'continuity' between river channels and bathyal slope channels was likely enhanced by the tidal flow in the rivers and by the weakness of the waves.

Sediment transport from shelf-edge to slope through shelf-edge deltas

The main drivers for how the system reacts as it crosses the shelf to the slope-break area involve: (**1**) base-level changes (eustatic or tectonic); and (**2**) regressions driven by mainly by climate and severe river flooding, operating on a faster timescale than base-level change.

1A. **Base-Level Change**: If relative sea level is reasonably rising (eustasy or high subsidence) the topset aggrades, the clinoform is continuous and smoothly sigmoidal. As the river discharges onto the slope break there is no chaos, no major collapsing but hyperconcentrated flows from the river channel (not necessarily hyperpycnal flows) become regular turbidity currents (low or high density) on the upper slope. This produces 'sigmoidal' clinoforms. Examples of this type of shelf–slope transition from Gulf of Corinth Gilbert Deltas (Gobo *et al.*, 2015) and from Tanqua Karoo (Dixon *et al.*, 2012a,b).

1B. **Base Level Change**: If relative sea level is falling (eustasy or tectonic uplift in the hinterland) the topset can be eroded by downcutting channels and there can be major collapsing and slumping at the slope break, so that predominant debris flows (cohesive or cohesionless) as well as slump masses and even blocks of collapsed shelf edge, pass onto the slope. Examples of this type of transition are from Gulf of Corinth Gilbert deltas (Gobo *et al.*, 2015), and the present Bey Malec clinoform in La Jardinera. However, there is no evidence for major collapsing and slumping at the slope-break deposits in the Bey Malec case, as already described.

2A. **Base-Level change rate $\ll$ cross-shelf delta migration rate**: Delta migration across shelf driven primarily by periodic flooding in the river system and not by changing base level. The topset–slope transition is similar to 1A above with river discharge of hyperpycnal flows transforming into high or low-density turbidites, without major collapsing. Clinoform is sigmoidal. Eventual sea-level rise is needed to start the next cycle. Examples of this type of shelf–slope transition are Spitsbergen Clinoforms 8 (Mellere *et al.*, 2003) and 14 (Petter & Steel, 2006) and possibly Karoo by Dixon *et al.* (2012, 2013), and the present Don Cordero clinoform in La Jardinera.

2B. **As in 2A, but conglomeratic river flows terminate before outermost shelf** and subaqueous sandy hyperpycnal flows produce fan lobes on the outer shelf, probably minimal sediment onto slope. An example of this can be found in Steel *et al.* (2018).

CONCLUSIONS

The Lower–Middle Jurassic Lajas and Los Molles formations in the Arroyo La Jardinera area, Neuquén Basin, Argentina, represent an unusual and well-exposed example of conglomeratic shelf-edge delta deposits, with the following main characteristics:

1 Pervasive channelization on the outer coastal plain and fronting river-dominated, tide-influenced deltas. There were wide distributary fairways with river-channel belts separated by inter-distributary sand belts near or at the shelf edge. Relatively strong tidal currents left their signals in the inter-distributary areas, but were

largely drowned out or reworked in the main fairways by the river flooding.

2 Lack of collapsed and slumped strata at the shelf edge suggest continuity between subaqueous river channels and deepwater slope channels. However, there is a marked contrast between the stratified and sorted framework gravels of the subaqueous delta channels and the sandy debris flows filling most of the middle to upper slope channels. The continuity is highlighted by some interfingering between these fluvial and debris-flow textures within uppermost slope-channel fills.

3 The interplay between flood tides and river currents, an autogenic process within deltas, is interpreted to have primarily modulated sediment bypass through preferential routes (i.e. distributary fairways) on the outer-shelf to shelf-edge and down onto the slope. Such focusing of river drainages at or near the shelf edge can be seen from seismic data sets, but has been rarely documented in outcrop studies.

4 Shelf to slope sediment transport in shelf-edge deltas can be seen to be primarily driven by the interplay between: (i) base-level changes (eustatic and tectonic); and (ii) regressions driven mainly by climate and severe river flooding, operating on a faster timescale than base-level changes. This association controls both how distributary systems build and link with slope systems, as well as large-scale shelf-margin morphology (for example, oblique versus sigmoidal clinoform sets, as interpreted for the La Jardinera case).

The documented shelf-edge delta deposits are an important contributor to the shelf-delta literature because of their unusual coarseness and tidal influence in the inter-distributary or distributary-abandoned areas. Additionally, they provide new examples on how delta distributary and slope channels link to bypass significant amounts of coarse-grained sediments onto deepwater areas of shelf margins.

ACKNOWLEDGEMENTS

The authors sincerely thank PlusPetrol, Shell and YPF for the financial and technical support during this research. We thank CAPES – Coordination for the Improvement and Training of Higher Education Personnel – for providing scholarship. This work was also funded by FAPERGS/CAPES through Notice 03/2018 – PRÓ-EQUIPAMENTOS (18/2551-0000429-4). We would like to thank the owners of the ranches for generously allowing land access, and Nestor Angelini for his assistance in Argentina. We thank The University of Texas at Austin and Universidade do Vale do Rio dos Sinos (Unisinos) for logistical, academic and technical support. This paper was remarkably improved by the constructive comments and critical review of Stephen Hubbard (University of Calgary), Peter Burgess (University of Liverpool) and one anonymous reviewer, as well as by the constructive editorial comments of Massimiliano Ghinassi.

REFERENCES

Ainsworth, R.B., **Vakarelov, B.K.**, **Lee, C.**, **MacEachern, J.A.**, **Montgomery, A.E.**, **Ricci, L.P.** and **Dashtgard, S.E.** (2015) Architecture and evolution of a regressive, tide-influenced marginal marine succession, Drumheller, Alberta, Canada. *J. Sed. Res.*, **85**, 596–625.

Archer, A.W. and **Hubbard, M.S.** (2003) Highest tides of the world. *Special Papers-Geological Society of Ameica*, 151–174.

Bouma, A.H. (1962) *Sedimentology of Some Flysch Deposits: A Graphic Approach to Facies Interpretation*. Elsevier, Amsterdam, 168 pp.

Brinkworth, W., **Vocaturo, G.**, **Loss, M.L.**, **Giunta, D.**, **Mortaloni, E.** and **Massaferro, J.L.** (2017) *Integración regional de subsuelo orientado a la exploración y desarrollo de Grupo Cuyo, Cuenca Neuquina*. Congreso Geológico Argentino, Tucumán.

Burgess, P.M. and **Hovius, N.** (1998) Rates of delta progradation during highstands: consequences for timing of deposition in deep-marine systems. *J. Geol. Soc.*, **155**, 217–222.

Burgess, P.M., **Flint, S.** and **Johnson, S.** (2000) Sequence stratigraphic interpretation of turbiditic strata: an example from Jurassic strata of the Neuquén basin, Argentina. *Geol. Soc. Am. Bull.*, **112**, 1650–1666.

Carter, R.M. (1975) A discussion and classification of subaqueous mass-transport with particular application to grain-flow, slurry-flow, and fluxoturbidites. *Earth Sci. Rev.*, **11**, 145–177.

Carvajal, C.R. and **Steel, R.J.** (2006) Thick turbidite successions from supply-dominated shelves during sea-level highstand. *Geology*, **34**, 665–668.

Covault, J.A., **Normark, W.R.**, **Romans, B.W.** and **Graham, S.A.** (2007) Highstand fans in the California borderland: the overlooked deep-water depositional systems. *Geology*, **35**, 783–786.

Covault, J.A., **Romans, B.W.** and **Graham, S.A.** (2009) Outcrop expression of a continental-margin-scale shelf-edge delta from the Cretaceous Magallanes Basin, Chile. *J. Sed. Res.*, **79**, 523–539.

Cummings, D.I., **Arnott, R.W.C.** and **Hart, B.S.** (2006) Tidal signatures in a shelf-margin delta. *Geology*, **34**, 249–252.

Dakin, N., **Pickering, K.T.**, **Mohrig, D.** and **Bayliss, N.J.** (2013) Channel-like features created by erosive submarine debris flows: field evidence from the Middle Eocene Ainsa Basin, Spanish Pyrenees. *Mar. Pet. Geol.*, **41**, 62–71.

Dalrymple, R.W. and **Choi, K.** (2007) Morphologic and facies trends through the fluvial–marine transition in tide-dominated depositional systems: a schematic framework for environmental and sequence-stratigraphic interpretation. *Earth Sci. Rev.*, **81**, 135–174.

Dalrymple, R.W. and **Rhodes, R.N.** (1995) Estuarine dunes and bars. In: *Geomorphology Sedimentology of Estuaries* (Ed. Perillo, G.M.E.). Amsterdam, Elsevier. Developments in sedimentology, **53**, 359–422.

Dixon, J.F., **Steel, R.J.** and **Olariu, C.** (2012a) River-dominated, shelf-edge deltas: delivery of sand across the shelf break in the absence of slope incision. *Sedimentology*, **59**, 1133–1157.

Dixon, J.F., **Steel, R.J.** and **Olariu, C.** (2012b) Shelf-edge delta regime as a predictor of deep-water deposition. *J. Sed. Res.*, **82**, 681–687.

Dzulynski, S., **Ksiazkiewicz, M.** and **Kuenen, P.H.** (1959) Turbidites in flysch of the Polish Carpathian Mountains. *Geol. Soc. Am. Bull.*, **70**, 1089–1118.

Dzulynski, S., **Radomski, A.** and **Slaczka, A.** (1957) Sandstone whirl-balls in the silts of the Carpathian flysch. *Ann. Soc. Géol. Pol.*, **26**, 107–126.

Fleming, R. and **Revelle, R.** (1939) Part 2. Relation of oceanography to sedimentation physical processes in the ocean. In: *Recent marine sediments: a symposium* (p. 48). The American Association of Petroleum Geologists.

Franzese, J.R. and **Spalletti, L.A.** (2001) Late Triassic–early Jurassic continental extension in southwestern Gondwana: tectonic segmentation and pre-break-up rifting. *J. S. Am. Earth Sci.*, **14**, 257–270.

Franzese, J., **Spalletti, L.**, **Pérez, I.G.** and **Macdonald, D.** (2003) Tectonic and paleoenvironmental evolution of Mesozoic sedimentary basins along the Andean foothills of Argentina (32–54 S). *J. S. Am. Earth Sci.*, **16**, 81–90.

Galloway, W.E. (1998) Siliciclastic slope and base-of-slope depositional systems: component facies, stratigraphic architecture, and classification. *AAPG Bull.*, **82**, 569–595.

Gan, Y.P., **Steel, R.J.**, **Olariu, C.** and **De Almeida, F.** (2019) Facies and architectural variability of sub-seismic slope-channel fills in prograding clinoforms, Mid-Jurassic Neuquén Basin, Argentina. *Basin Res.*

Gobo, K., **Ghinassi, M.** and **Nemec, W.** (2015) Gilbert-type deltas recording short-term base-level changes: delta-brink morphodynamics and related foreset facies. *Sedimentology*, **62**, 1923–1949.

Gomis-Cartesio, L.E., **Poyatos-More, M.**, **Flint, S.S.**, **Hodgson, D.M.**, **Brunt, R.L.** and **Wickens, H.V.** (2016) Anatomy of a mixed-influence shelf-edge delta, Karoo Basin, South Africa. *Geol. Soc. Spec. Publ.*, **444**, 393–418.

Gomis-Cartesio, L.E., **Poyatos-Moré, M.**, **Hodgson, D.M.** and **Flint, S.S.** (2018) Shelf-margin clinothem progradation, degradation and readjustment: Tanqua depocentre, Karoo Basin (South Africa). *Sedimentology*, **65**, 809–841.

Gugliotta, M., **Flint, S.S.**, **Hodgson, D.M.** and **Veiga, G.D.** (2015) Stratigraphic record of river-dominated crevasse subdeltas with tidal influence (Lajas Formation, Argentina). *J. Sed. Res.*, **85**, 265–284.

Gulisano, C.A. and **Pando, G.A.** (1981) Estratigrafía y facies de los depósitos jurásicos entre Piedra del Águila y Sañicó, Departamento Collón Curá, Provincia del Neuquén. *Congr. Geol. Argentino*, **8**, 553–577.

Gulisano, C.A., **Gutiérrez Pleimling, A.R.** and **Digregorio, R.E.** (1984) Esquema estratigráfico de la secuencia jurásica del oeste de la provincia del Neuquén. *Congreso Geológico Argentino*, 236–259.

Harms, J.C., **Southard, J.B.** and **Walker, R.G.** (1982) Shallow marine environments-a comparison of some ancient and modern examples. In: *Structures and Sequences in Clastic Rocks. Lecture Notes from Short Course No 9* (Eds Harms, J.C., Southard, J.B. and Walker, R.G.), Society of Economic Paleontologists and Mineralogists.

Hernández-Molina, F.J., **Fernández-Salas, L.M.**, **Lobo, F.**, **Somoza, L.**, **Díaz-del-Río, V.** and **Dias, J.A.** (2000) The infralittoral prograding wedge: a new large-scale progradational sedimentary body in shallow marine environments. *Geo-Mar. Lett.*, **20**, 109–117.

Hoitink, A.J.F., **Wang, Z.B.**, **Vermeulen, B.**, **Huismans, Y.** and **Kästner, K.** (2017) Tidal controls on river delta morphology. *Nat. Geosci.*, **10**, 637–645.

Houseknecht, D.W., **Bird, K.J.** and **Schenk, C.J.** (2009) Seismic analysis of clinoform depositional sequences and shelf-margin trajectories in Lower Cretaceous (Albian) strata, Alaska North Slope. *Basin Res.*, **21**, 644–654.

Howell, J.A., **Schwarz, E.**, **Spalletti, L.A.** and **Veiga, G.D.** (2005) The Neuquén basin: an overview. *Geol. Soc. London Spec. Publ.*, **252**, 1–14.

Hubbard, S.M., **Fildani, A.**, **Romans, B.W.**, **Covault, J.A.** and **McHargue, T.R.** (2010) High-relief slope clinoform development: insights from outcrop, Magallanes Basin, Chile. *J. Sed. Res.*, **80**, 357–375.

Hubbard, S.M., **Covault, J.A.**, **Fildani, A.** and **Romans, B.W.** (2014) Sediment transfer and deposition in slope channels: deciphering the record of enigmatic deep-sea processes from outcrop. *Geol. Soc. Am. Bull.*, **126**, 857–871.

Introcaso, A., **Pacino, M.C.** and **Fraga, H.** (1992) Gravity, isostasy and Andean crustal shortening between latitudes 30 and 35 S. *Tectonophysics*, **205**, 31–48.

Johannessen, E.P. and **Steel, R.J.** (2005) Shelf-margin clinoforms and prediction of deepwater sands. *Basin Res.*, **17**, 521–550.

Jones, G.E., **Hodgson, D.M.** and **Flint, S.S.** (2015) Lateral variability in clinoform trajectory, process regime, and sediment dispersal patterns beyond the shelf-edge rollover in exhumed basin margin-scale clinothems. *Basin Res.*, **27**6, 657–680.

Kenyon, N.H., **Belderson, R.H.**, **Stride, A.H.** and **Johnson, M.A.** (1981) Offshore tidal sand banks as indicators of net sand transport and as potential deposits. *Holocene Mar. Sediment. North Sea Basin*, **5**, 257–268.

Kim, Y., **Kim, W.**, **Cheong, D.**, **Muto, T.** and **Pyles, D.R.** (2013) Piping coarse-grained sediment to a deep water fan through a shelf-edge delta bypass channel: tank experiments. *J. Geophys. Res., series F*, **118**, 2279–2291.

Kim, H.J., **Mallea, M.**, **Gutiérrez, R.** and **Malone, P.** (2014) Exploracion del Gr. Cuyo Jurasico en Bloques Maduros de la Dorsal Huincul – puesto touquet y el Porvenir, Quenca Neuquena. *IX Congreso de Exploración y Desarrollo de Hidrocarburos*, Mendoza-Argentina, 2, pag. 71–93.

Kochhann, K.G.D., **Baecker-Fauth, S.**, **Pujana, I.**, **da Silveira, A.S.** and **Fauth, G.** (2011) Toarcian-Aalenian (Early–Middle Jurassic) radiolarian fauna from the Los Molles Formation, Neuquén Basin, Argentina: taxonomy and paleobio-
geographic affinities. *J. S. Am. Earth Sci.*, **31**, 253–261.

Kurcinka, C., **Dalrymple, R.W.** and **Gugliotta, M.** (2018) Facies and architecture of river-dominated to tide-influenced mouth bars in the lower Lajas Formation (Jurassic), Argentina. *AAPG Bull.*, **102**, 885–912.

Laugier, F.J. and **Plink-Björklund, P.** (2016) Defining the shelf edge and the three-dimensional shelf edge to slope facies

variability in shelf-edge deltas. *Sedimentology*, **63**, 1280–1320.

Legarreta, L. and **Gulisano, C.A.** (1989) Análisis estratigráfico secuencial de la Cuenca Neuquina (Triásico superior-Terciario inferior, Argentina). In: *Cuencas Sedimentarias Argentinas* (Eds Chebli, G. and Spalletti, L.), Serie Correlación Geológica, Universidad Nacional de Tucumán, **6**, 221–243.

Legarreta, L. and **Uliana, M.A.** (1991) Jurassic-Cretaceous marine oscillations and geometry of back arc basin fill, Central Argentine Andes. In: *Sedimentation, Tectonics and Eustasy- Sea-level Changes at Active Margins* (Ed. **Macdonald, D.I.M.**), International Association of Sedimentologists, Special Publications, **12**, 429–450.

Legarreta, L. and **Uliana, M.A.** (1996) The Jurassic succession in west-central Argentina: stratal patterns, sequences and paleogeographic evolution. *Palaeogeogr. Palaeoclimatol. Palaeoecol.*, **120**, 303–330.

Leuven, J.R., **van Maanen, B.**, **Lexmond, B.R.**, **van der Hoek, B.V.**, **Spruijt, M.J.** and **Kleinhans, M.G.** (2018) Dimensions of fluvial-tidal meanders: are they disproportionally large? *Geology*, **46**, 923–926.

Liu, Z.X. (1997) Yangtze Shoal—a modern tidal sand sheet in the northwestern part of the East China Sea. *Mar. Geol.*, **137**, 321–330.

Longhitano, S.G., **Mellere, D.**, **Steel, R.J.** and **Ainsworth, R.B.** (2012) Tidal depositional systems in the rock record: a review and new insights. *Sed. Geol.*, **279**, 2–22.

Lowe, D.R. (1982) Sediment gravity flows: II Depositional models with special reference to the deposits of high-density turbidity currents. *J. Sed. Res.*, **52**, 279–297.

Manceda, R. and **Figueroa, D.** (1995) Inversion of the Mesozoic Neuquén rift in the Malargüe fold and thrust belt, Mendoza, Argentina. In: *Petroleum Basins of South America* (Eds Tankard, A.J., Suaréz Soruco, R. and Welsink, H.J.), AAPG Memoirs, **62**, 369–382.

McIlroy, D., **Flint, S.**, **Howell, J.A.** and **Timms, N.** (2005) Sedimentology of the tide-dominated Jurassic Lajas Formation, Neuquén Basin, Argentina. *Geol. Soc. London Spec. Publ.*, **252**, 83–107.

Mellere, D., **Plink-Björklund, P.** and **Steel, R.** (2002) Anatomy of shelf deltas at the edge of a prograding Eocene shelf margin, Spitsbergen. *Sedimentology*, **49**, 1181–1206.

Mellere, D., **Breda, A.**, **Steel, R.J.**, **Roberts, H.H.**, **Rosen, N.C.**, **Fillon, R.H.** and **Anderson, J.B.** (2003) Fluvially-incised shelf-edge deltas and linkage to upper-slope channels (Central Tertiary Basin, Spitsbergen). *Global significance and future exploration potential: Gulf Coast Section-SEPM Special Publication*, **23**, 231–266.

Mitchum, R.M., Jr, **Vail, P.R.** and **Thompson, S., III** (1977) Seismic stratigraphy and global changes of sea level, Part 2. The depositional sequence as a basic unit for stratigraphic analysis. *AAPG Bull.*, **26**, 53–62.

Moscardelli, L., **Wood, L.** and **Mann, P.** (2006) Mass-transport complexes and associated processes in the offshore area of Trinidad and Venezuela. *AAPG Bull.*, **90**, 1059–1088.

Moss-Russell, A.C. (2009) The stratigraphic architecture of a prograding shelf-margin delta in outcrop, the Sobrarbe Formation, Ainsa Basin, Spain. Master's Thesis, Colorado School of Mines, 192 pp.

Nemec, W. and **Steel, R.J.** (1984) Alluvial and coastal conglomerates: their significant features and some comments on gravelly mass-flow deposits. In: *Sedimentology of Gravels and Conglomerates* (Eds Koster, E.H. and Steel, R.J.), Canadian Society of Petroleum Geologists Memoir, **10**, 1–31. .

Olariu, C., **Steel, R.J.**, **Dalrymple, R.W.** and **Gingras, M.K.** (2012a) Tidal dunes versus tidal bars: the sedimentological and architectural characteristics of compound dunes in a tidal seaway, the lower Baronia Sandstone (Lower Eocene), Ager Basin, Spain. *Sed. Geol.*, **279**, 134–155.

Olariu, M.I., **Olariu, C.**, **Steel, R.J.**, **Dalrymple, R.W.** and **Martinius, A.W.** (2012b) Anatomy of a laterally migrating tidal bar in front of a delta system: Esdolomada Member, Roda Formation, Tremp-Graus Basin, Spain. *Sedimentology*, **59**, 356–378.

Olariu, C., **Steel, R.J.**, **Vann, N.**, **Tudor, E.**, **Shin, M.**, **Winter, R.**, **Gan, Y.**, **Jung, E.**, **Almeida, F.**, **Minisini, D.**, **Brinkworth, W.**, **Loss, L.**, **Inigo, J.** and **Gutierrez, R.** (2019) Criteria for recognition of shelf-slope clinoforms using outcrop data; Jurassic Lajas and Los Molles formations, S. Neuquén Basin, Argentina. *Basin Res.*

Paim, P.S., **Silveira, A.S.**, **Lavina, E.L.**, **Faccini, U.F.**, **Leanza, H.A.**, **de Oliveira, J.T.** and **D'Avila, R.S.** (2008) High resolution stratigraphy and gravity flow deposits in the Los Molles Formation (Cuyo Group, Jurassic) at La Jardinera region, Neuquén Basin. *Rev. Asoc. Geol. Argentina*, Simposio Jurásico de América del Sur, **63**, 728–753.

Paim, P.S.G., **Lavina, E.L.C.**, **Faccini, U.F.**, **Silveira, A.S.**, **Leanza, H.** and **D'Avila, R.S.F.** (2011) Fluvial-derived turbidites in the Los Molles Formation (Jurassic of the Neuquen Basin): initiation, transport, and deposition. In: *Sediment Transfer from Shelf to Deep Water—Revisiting the Delivery System* (Eds Slatt, R.M. and Zavala, C.), AAPG Studies in Geology, **61**, 95–116.

Patruno, S. and **Helland-Hansen, W.** (2018) Clinoforms and clinoform systems: review and dynamic classification scheme for shorelines, subaqueous deltas, shelf edges and continental margins. *Earth Sci. Rev.*, **185**, 202–233.

Paumard, V., **Bourget, J.**, **Payenberg, T.**, **Ainsworth, B.**, **Lang, S.**, **Posamentier, H.** and **George, A.** (2018) Shelf-margin architecture and shoreline processes at the shelf-edge: controls on sediment partitioning and prediction of deep-water deposition style. *ASEG Extend. Abstracts*, **2018**, 1–6.

Peng, Y., **Steel, R.J.** and **Olariu, C.** (2017) Transition from storm wave-dominated outer shelf to gullied upper slope: the mid-Pliocene Orinoco shelf margin, South Trinidad. *Sedimentology*, **64**, 1511–1539.

Perov, G. and **Bhattacharya, J.P.** (2011) Pleistocene shelf-margin delta: intradeltaic deformation and sediment bypass, northern Gulf of Mexico. *AAPG Bull.*, **95**, 1617–1641.

Petter, A.L. and **Steel, R.J.** (2006) Hyperpycnal flow variability and slope organization on an Eocene shelf margin, Central Basin, Spitsbergen. *AAPG Bull.*, **90**, 1451–1472.

Plink-Björklund, P. (2012) Effects of tides on deltaic deposition: causes and responses. *Sed. Geol.*, **279**, 107–133.

Plink-Björklund, P. and **Steel, R.J.** (2004) Initiation of turbidity currents: outcrop evidence for Eocene hyperpycnal flow turbidites. *Sed. Geol.*, **165**, 29–52.

Plink-Björklund, P. and **Steel, R.** (2005) Deltas on falling-stage and lowstand shelf margins, the Eocene Central Basin of Spitsbergen: importance of sediment supply. In: *River Deltas—Concepts, Models, and Examples* (Eds Giosan, L. and Bhattacharya, J.P.), *SEPM Spec. Publ.*, **83**, 179–206.

Porebski, S.J. and **Steel, R.J.** (2003) Shelf-margin deltas: their stratigraphic significance and relation to deepwater sands. *Earth-Sci. Rev.*, **62**, 283–326.

Postma, G., **Cartigny, M.** and **Kleverlaan, K.** (2009) Structureless, coarse-tail graded Bouma Ta formed by internal hydraulic jump of the turbidity current? *Sed. Geol.*, **219**, 1–6.

Postma, G., **Nemec, W.** and **Kleinspehn, K.L.** (1988) Large floating clasts in turbidites: a mechanism for their emplacement. *Sed. Geol.*, **58**, 47–61.

Poyatos-Moré, M., **Jones, G.D.**, **Brunt, R.L.**, **Hodgson, D.M.**, **Wild, R.J.** and **Flint, S.S.** (2016) Mud-dominated basin-margin progradation: processes and implications. *J. Sed. Res.*, **86**, 863–878.

Pyles, D.R. and **Slatt, R.M.** (2007) Applications to understanding shelf edge to base-of-slope changes in stratigraphic architecture of prograding basin margins: stratigraphy of the Lewis Shale, Wyoming, USA. In: *Atlas of Deep-water Outcrops* (Eds Nilsen, T.H., Shew, R.D., Steffens, G.S. and Strudlick, J.R.J.), AAPG Studies in Geology, **56**, CD-ROM, 1–19.

Ramos, V. (1999) Plate tectonic setting of the Andean Cordillera. *Episodes*, **22**, 183–190.

Reid, W. and **Patruno, S.** (2015) The East Shetland Platform: unlocking the platform potential. With significant advancements in seismic acquisition technology, it is time to re-visit the East Shetland Platform. *GeoExpro*, **12**, 41–46.

Reynaud, J.Y. and **Dalrymple, R.W.** (2011) Shallow-marine tidal deposits. In: *Principles of Tidal Sedimentology*(Eds. Davis, R.A., Jr and Dalrymple, R.W.), pp. 335–369. Springer, Dordrecht.

Riccardi, A.C., **Leanza, H.A.**, **Damborenea, S.E.**, **Manceñido, M.O.**, **Ballent, S.C.** and **Zeiss, A.** (2000) Marine mesozoic biostratigraphy of the Neuquén basin. *Z. Angew. Geol.*, **1**, 102–108.

Ross, W.C., **Watts, D.E.** and **May, J.A.** (1995) Insights from stratigraphic modeling: mud-limited versus sand-limited depositional systems. *AAPG Bull.*, **79**, 231–258.

Rossi, V.M. and **Steel, R.J.** (2016) The role of tidal, wave and river currents in the evolution of mixed-energy deltas: example from the Lajas Formation (Argentina). *Sedimentology*, **63**, 824–864.

Ryan, M.C., **Helland-Hansen, W.**, **Johannessen, E.P.** and **Steel, R.J.** (2009) Erosional vs. accretionary shelf margins: the influence of margin type on deepwater sedimentation: an example from the Porcupine Basin, offshore western Ireland. *Basin Res.*, **21**, 676–703.

Sassi, M.G., **Hoitink, A.J.F.**, **de Brye, B.** and **Deleersnijder, E.** (2012) Downstream hydraulic geometry of a tidally influenced river delta. *J. Geophys. Res.*, **117**, 676.

Schwartz, T.M. and **Graham, S.A.** (2015) Stratigraphic architecture of a tide-influenced shelf-edge delta, Upper Cretaceous Dorotea Formation, Magallanes-Austral Basin, Patagonia. *Sedimentology*, **62**, 1039–1077.

Shanmugam, G. (1996) High-density turbidity currents; are they sandy debris flows? *J. Sed. Res.*, **66**, 2–10.

Shchepetkina, A., **Gingras, M.K.**, **Mángano, M.G.** and **Buatois, L.A.** (2019) Fluvio-tidal transition zone: terminology, sedimentological and ichnological characteristics, and significance. *Earth Sci. Rev.*, **192**, 214–235.

Silalahi, H. (2009) Stratigraphic architecture of slope deposits associated with prograding margins, Sobrarbe Formation: Ainsa Basin, Spain. Master's Thesis, Colorado School of Mines, Golden, CO, 146 pp.

Souza, A.J., **Alvarez, L.G.** and **Dickey, T.D.** (2004) Tidally induced turbulence and suspended sediment. *Geophys. Res. Lett.*, **31**, 1–5.

Steckler, M.S., **Mountain, G.S.**, **Miller, K.G.** and **Christie-Blick, N.** (1999) Reconstruction of Tertiary progradation and clinoform development on the New Jersey passive margin by 2-D backstripping. *Mar. Geol.*, **154**, 399–420.

Steel, R.J. and **Olsen, T.** (2002) Clinoforms, clinoform trajectories and deepwater sands. In: *Sequence Stratigraphic Models for Exploration and Production: evolving Methodology, Emerging Models and Application Histories* (Eds Armentrout, J.M. and Rosen, N.C.), GCS-SEMP Found 22nd Annu Res Conf Proc, 367–381(CD-ROM).

Steel, R.J., **Crabaugh, J.**, **Schellpeper, M.**, **Mellere, D.**, **Plink-Bjorklund, P.**, **Deibert, J.** and **Loeseth, T.** (2000) Deltas vs. rivers on the shelf edge: their relative contributions to the growth of shelf-margins and basin-floor fans (Barremian and Eocene, Spitsbergen). *Deepwater Reserv. World*, **15**, 981–1009.

Steel, E., **Simms, A.R.**, **Steel, R.** and **Olariu, C.** (2018) Hyperpycnal delivery of sand to the continental shelf: insights from the Jurassic Lajas Formation, Neuquén Basin, Argentina. *Sedimentology*, **65**, 2149–2170.

Steel, R.J., **Olariu, C.**, **Zhang, J.** and **Chen, S.** (2019) What is the topset of a shelf prism? *Basin Res. Spec. Publ.* (in press).

Stow, D.A.V. and **Piper, D.J.W.** (1984) Deep-water fine-grained sediments: facies models. *Geol. Soc. London Spec. Publ.*, **15**, 611–646.

Stride, A.H. (1982) Offshore tidal deposits: sand sheet and sand bank facies. In: *Offshore Tidal Sands* (Ed. Stride, A.H.), pp. 95–125. Springer, Dordrecht.

Sydow, J. and **Roberts, H.H.** (1994) Stratigraphic framework of a late Pleistocene shelf-edge delta, northeast Gulf of Mexico. *AAPG Bull.*, **78**, 1276–1312.

Sylvester, Z., **Deptuck, M.E.**, **Prather, B.E.**, **Pirmez, C.** and **O'Byrne, C.** (2012) Seismic stratigraphy of a shelf-edge delta and linked submarine channels in the northeastern Gulf of Mexico. In: *Application of the Principles of Seismic Geomorphology to Continental-Slope and Base-of-slope Systems: Case Studies from Seafloor and Near-Seafloor Analogues* (Eds Prather, B., Deptuck, M.E., Mohrig, C., Van Hoor, B. and Wynn, R.B.), SEPM Society for Sedimentary Geology Special Publication, **99**, 31–59.

Tooth, S. and **McCarthy, T.S.** (2004) Controls on the transition from meandering to straight channels in the wetlands of the Okavango Delta, Botswana. *Earth Surf. Proc. Land.*, The Journal of the British Geomorphological Research Group, **29**, 1627–1649.

Uliana, M.A., **Biddle, K.T.** and **Cerdan, J.** (1989) Mesozoic extension and the formation of argentine sedimentary basins: chapter 39: analogs. 599–614.

Uroza, C.A. and **Steel, R.J.** (2008) A highstand shelf-margin delta system from the Eocene of West Spitsbergen, Norway. *Sed. Geol.*, **203**, 229–245.

Veiga, G.D. (2000) Estratigrafía y Sedimentología de la Formación Challacó, Cuenca Neuquina Austral, República Argentina. Doctoral dissertation, Universidad Nacional de La Plata.

Vergani, G.D., **Tankard, A.J.**, **Belotti, H.J.** and **Welsink, H.J.** (1995) Tectonic evolution and paleogeography of the Neuquén Basin, Argentina. In: *Petroleum Basins of South America* (Eds Tankard, A.J., Suaréz Soruco, R. and Welsink, H.J.), AAPG Memoirs, **62**, 383–402.

Zavala, C. (1993) Estratigrafía y análisis de facies de la Formación Lajas (Jurásico medio) en el sector suroccidental de la Cuenca Neuquina. Provincia del Neuquén. República Argentina. Doctoral Dissertation, Universidad Nacional del Sur.

Zavala, C. (1996a) Sequence stratigraphy in continental to marine transitions. An example from the Middle Jurassic Cuyo Group, south Neuquén Basin, Argentina. *GeoResearch Forum*, **1**, 285–293.

Zavala, C. (1996b) High-resolution sequence stratigraphy in the Middle Jurassic Cuyo Group, South Neuquén Basin, Argentina. *GeoResearch Forum*, **1**, 295–303.

Zavala, C. and **González, R.** (2001) Estratigrafia del Grupo Cuyo (Jurásico inferior-medio) en la Sierra de la Vaca Muerta, cuenca Neuquina. *Bol. Inform. Petrol.*, **65**, 40–54.

Manuscript received 9 March 2019; revision accepted 12 February 2020